NASA Technical Memorandum 110370

# Acoustic Flight Tests of Rotorcraft Noise-Abatement Approaches Using Local Differential GPS Guidance

Robert T. N. Chen, William S. Hindson, and Arnold W. Mueller

September 1995


National Aeronautics and
Space Administration

NASA Technical Memorandum 110370

# Acoustic Flight Tests of Rotorcraft Noise-Abatement Approaches Using Local Differential GPS Guidance

Robert T. N. Chen and William S. Hindson, Ames Research Center, Moffett Field, California
Arnold W. Mueller, Langley Research Center, Hampton, Virginia

September 1995


National Aeronautics and
Space Administration

**Ames Research Center**
Moffett Field, California 94035-1000

# Acoustic Flight Tests of Rotorcraft Noise-Abatement Approaches Using Local Differential GPS Guidance

ROBERT T. N. CHEN, WILLIAM S. HINDSON, AND ARNOLD W. MUELLER*

*Ames Research Center*

## Summary

This paper presents the test design, instrumentation set-up, data acquisition, and the results of an acoustic flight experiment to study how noise due to blade-vortex interaction (BVI) may be alleviated. The flight experiment was conducted using the NASA/Army Rotorcraft Aircrew Systems Concepts Airborne Laboratory (RASCAL) research helicopter. A Local Differential Global Positioning System (LDGPS) was used for precision navigation and cockpit display guidance. A laser-based rotor state measurement system on board the aircraft was used to measure the main rotor tip-path-plane angle-of-attack. Tests were performed at Crows Landing Airfield in northern California with an array of microphones similar to that used in the standard ICAO/FAA noise certification test. The methodology used in the design of a RASCAL-specific, multi-segment, decelerating approach profile for BVI noise abatement is described, and the flight data pertaining to the flight technical errors and the acoustic data for assessing the noise reduction effectiveness are reported.

## Nomenclature

| | |
|---|---|
| $a$ | acceleration, ft/s$^2$ |
| $C_T$ | thrust coefficient |
| $D$ | diameter of the main rotor, ft |
| $g$ | gravitational acceleration, ft/s$^2$ |
| $i_s$ | inherent shaft tilt angle, deg |
| $r$ | distance from the rotor hub center to the microphone, ft |
| $t$ | time, sec |
| $v_h$ | hover mean induced velocity (normalized with tip speed) |
| $v_T$ | normalized total velocity at the rotor disc center, $v_T = \left(\mu^2 + \lambda^2\right)^{1/2}$ |
| $V$ | airspeed, knots (or ft/s) |
| $V_\infty$ | free-stream or flight velocity of the aircraft (normalized with tip speed) |
| $\dot{V}$ | acceleration along the flightpath, ft/s$^2$ |
| $x$ | horizontal distance from the center ground microphone (positive forward), ft |
| $z$ | vertical distance from the center ground microphone (positive downward), ft |
| $\alpha$ | aircraft angle of attack, deg |
| $\theta$ | aircraft pitch attitude, deg |
| $\gamma_{s.s.}$ | quasi-steady flightpath angle, deg |
| $\gamma_{eff}$ | effective glidepath angle, deg |
| $\beta_{ic}$ | cosine component of the blade flapping in nonrotating system, deg |
| $\beta_{is}$ | sine component of the blade flapping in nonrotating system, deg |
| $\sigma$ | rotor solidity ratio |
| $\lambda$ | inflow ratio |
| $\mu$ | advance ratio |
| $\chi$ | wake skew angle, deg |
| BVI | Blade Vortex Interaction |
| EPNL | Effective perceived noise level |
| FAA | Federal Aviation Administration |
| HAI | Helicopter Association International |
| ICAO | International Civil Aviation Organization |
| LDGPS | Local Differential Global Positioning System |
| RASCAL | Rotorcraft Aircrew Systems Concepts Airborne Laboratory |

*Langley Research Center, Hampton, Virginia.

| | |
|---|---|
| SEL | Sound exposure level |
| TPP | Tip path plane |

## Introduction

It has been recognized that community noise is a major barrier to the full utilization of rotorcraft in an integrated air transportation system. One of the most significant sources of the noise generated by a passing, overflying, or approaching helicopter occurs when a rotor blade encounters the vortices shed by preceding blades. The phenomenon is known as blade-vortex interaction (BVI). It is characterized by an impulsive noise, sometimes called blade slap, which can be particularly objectionable during the descent to landing.

Solutions to the BVI noise problem lie both in design improvements to the rotor system and in the use of special flight procedures that avoid operation in conditions that are particularly conducive to BVI. The noise reduction improvements in the rotor system design include appropriate selection of blade tip speed, number of blades, disc loading, blade loading, blade tip geometry, and the use of active on-the-blade control schemes.

The use of special flight procedures, which are of primary interest in this paper, are known to helicopter pilots but they are difficult to fly with the necessary navigational precision even in visual flight conditions. Furthermore, there is presently no capability to adequately tailor approach operations for noise reduction in instrument flight conditions. Hence, even if these operational procedures can be proven effective for noise reduction, no credit for their use can be envisaged without the means to accurately and repeatably fly these approach profiles routinely in all weather conditions. The increasingly broad applications of the Local Differential Global Positioning System (LDGPS) to civilian aviation now makes this possible, thus opening the way to greater penetration of rotorcraft into the urban transportation infrastructure, as depicted schematically in figure 1.

Flight tests were undertaken in the summer of 1994 using the NASA/Army Rotorcraft Aircrew Systems Concepts Airborne Laboratory (RASCAL) research helicopter with its recently developed LDGPS-based cockpit display capabilities. These tests were conducted jointly with the FAA and addressed primarily the operational and piloting issues associated with the precision tracking of the prescribed multi-segment decelerating approach profiles using the LDGPS-based cockpit display guidance. Two generic approach flight profiles were tested which were defined according to the procedures contained in the Fly Neighborly Guide (ref. 1) published by the Helicopter Association International (HAI). The implementation, conduct, and results of the flight tests have been reported in reference 2. The ease and accuracy with which these approaches could be flown offered encouragement to pursue further this method of noise reduction.

Subsequently, a specific noise-abatement profile tailored to avoid the BVI-intensive region of the RASCAL research helicopter was designed based on acoustic data from wind-tunnel tests (refs. 3–5) and from flight tests (refs. 6 and 7) that were available for this type of helicopter. Acoustic tests were then conducted jointly by NASA Ames and Langley Research Centers at Crows Landing Airfield, approximately 50 miles east of Moffett Field, Calif., in January 1995. A precision laser tracking facility at the airfield was used to assess the navigational accuracy of the LDGPS. A microphone array similar to that used in the standard ICAO/FAA noise certification test (ref. 8) was set up to assess the noise reduction effectiveness of this specific noise-abatement profile. Generic HAI approach profiles appropriate to light and medium helicopters were also tested for acoustic reduction effectiveness. Additionally, three conventional descending approaches, namely 9 deg decelerating, 6 deg decelerating, and 6 deg constant speed at 80 knots, were also flown for the purpose of comparing the noise characteristics due to decelerating and flying single- and multi-segment approach profiles. Details of the design of the approach profiles for BVI noise abatement, the methods used to implement and conduct the test flights, and the results of the flight experiment are discussed in the following sections.

## Design of Approach Flight Profiles

Two generic noise-abatement approach profiles, “HAI-Light” and “HAI-Medium” which were adapted from a previous experiment (ref. 2), and a RASCAL-specific approach profile designed with an intention to reduce BVI noise of the RASCAL research helicopter, called “Quiet,” were flown in the acoustic flight tests. These three approach profiles are shown respectively in figures 2(a)–2(c). The HAI-Light and HAI-Medium were designed based on the HAI’s Fly Neighborly Guide (ref. 1). The detailed methodology used in the construction of these two generic profiles is described in reference 2. It involves the simultaneous consideration of many factors including obstacle clearance planes, clearway to the landing zone, minimum IFR airspeeds, one-engine-inoperative (OEI) performance for continued or balked landing, approved minimum altitudes in instrument flight conditions, and maximum scheduled rates of descent. The procedure used in the construction of the

RASCAL-specific BVI noise-abatement profile is described in the following paragraphs.

First, the ground noise footprints (refs. 6 and 7) generated from the measured ground-plane BVI acoustic data, which were collected with a large array of microphones for a variety of unaccelerated approach flights of a helicopter similar to RASCAL, were compiled and scored. A sample set of ground-plane noise-footprint contours for approach flights is presented in figures 3(a)–3(f). Figures 3(a)–3(c) show these EPNL (effective perceived noise level) footprints for the glide slopes of 6, 9, and 12 deg at the constant approach airspeed of 80 knots. Figures 3 (d)–3(f) present the noise contours for the airspeeds of 60, 80, and 100 knots at the constant glide slope of 9 deg. Acoustic data were not available for decelerating approach flights to enable an assessment of the effect of deceleration. A scale of 1 to 10 (from least to most noisy) was used to score subjectively the noise intensity in combination with the area of coverage. The result is shown in figure 4 for the various test conditions expressed in the plane of airspeed and rate of descent. To improve the consistency of scoring, several scorers were used. It can be seen that the noise-intensive region lies in the high speed-steep glide slope area with a rate of descent in excess of 1200 fpm, which is considered to be outside of the maximum operationally desirable value of 900 fpm as indicated in the figure.

Next, the RASCAL-specific noise-abatement approach profile, which was given the name “Quiet” for this flight experiment, was defined on the plane of airspeed and descent rate to avoid the BVI noise intensive region. In addition to the maximum acceptable rate of descent for assuring the comfort of the crew and passengers, other factors similar to those described above for defining the HAI-Light and HAI-Medium profiles (ref. 2), such as minimum IFR airspeeds and OEI operational requirements, were simultaneously considered to judiciously define the Quiet approach profile shown in figure 4.

The Quiet approach profile devised from the full scale flight acoustic data was briefly assessed using some available wind tunnel data to see whether the acoustic data from the two sources were consistent. To this end, a set of pertinent accoustic data of the 1/6 scale model of a main rotor similar to that of the RASCAL, which were obtained in the NASA Langley 14- by 22-Foot Subsonic Wind Tunnel (ref. 3), were assembled and plotted on the plane of descent rate vs. airspeed. Figure 5 shows the BVI noise contours from two strategically located microphones, namely a center stand microphone (azimuth angle = 177 deg; elevation angle = –23 deg; r/D = 1.505), and a starboard floor microphone (azimuth angle = 133 deg; elevation angle = –25 deg; r/D =1.4). There was no port side microphone comparable with the starboard one to assess the effect of directivity in this set of data. The airspeed and glide slope corresponding to this set of data are also somewhat limited; the data cover only the airspeed range of 50 to 80 knots and glide slope of up to 10 deg. These data were taken at the test condition of $CT/\sigma = 0.086$. The maximum noise level at the starboard mic is somewhat higher than that at the center mic even after adjustment for the distance discrepancy (about 0.63 dB). Within the range of airspeed and rate of descent, the noise contours at the starboard mic seem to be somewhat consistent with the flight acoustic data shown in figure 4. When plotted on figure 5 with the Quiet approach profile, consistency appears to be reasonable for the starboard microphone noise-contours, although less obvious based on the noise contours of the center microphone.

Another set of 1/6 scale model acoustic data (refs. 4 and 5) that were obtained from the Duits-Netherlandse Windtunnel (DNW) for a rotor similar to that of the test helicopter was also used for comparison with the flight test acoustic data. This set of data, taken at the test condition of $CT/\sigma = 0.07$, covers a broader range of airspeed as shown in figure 6 for three microphone locations. The azimuth location of these microphones was: 180 deg for the center microphone, 150 deg for the starboard microphone, and 210 deg for the port microphone. The elevation angle and the distance from the rotor hub center are the same for the three microphones, namely –25 deg and r/D = 1.50 respectively. These microphone locations were selected for the purpose of comparing with the selected microphones in the Langley tunnel described earlier. The acoustic data were processed with a passband of 500 to 3000 Hz to capture the dominant BVI noise, similar to that used in the Langley tunnel data described above. The directivity effect of the BVI noise is strong as evident from figures 6(b) and 6(c). The difference in the BVI noise between the starboard microphone and the port microphone exceeds 10 dB at some flight conditions. However, this set of data shows considerably smaller variation in noise level than the other wind tunnel data, as evident from comparing figure 5(a) with figure 6(a), and figure 5(b) with figure 6(b), especially in the critical speed range of 50 to 80 knots. There is no clear region with noticeably intensive BVI noise for this set of data. Also, lack of data in the low rate of descent region at the airspeed of 50 to 80 knots prevents an assessment of the Quiet profile in that region. However, the approach profile appears to be reasonable for the higher speed segment of 80 to 110 knots as evident from figure 6.

Finally to complete the definition of the Quiet approach profile, the level of deceleration was defined, and the

velocity and altitude profiles, expressed in terms of distance to the helipad, were calculated using

$$dz = [f(V)/V]\, dx \quad (1)$$

$$dV = [a/V]\, dx \quad (2)$$

where f(V) is the defined functional relationship between the rate of descent and airspeed for BVI noise-abatement shown in figure 4, and "a" is the level of constant deceleration. A value of 0.7 to 1 knot per second (0.035 to 0.05 g) was selected from handling qualities considerations. Beginning at the helipad, the integration is performed in a backward piecewise fashion, commensurate with the piecewise linear nature of the f(V) relationship. Operational constraints were incorporated in the process, including consideration of extended segments of the profile necessary to obtain desired initial path acquisition altitudes or airspeeds. Example constraints that were considered to define the integration limits were: (1) terminal speed at the helipad is zero, and (2) airspeed at decision height should be close to the takeoff safety speed, typically around 35–40 knots, thus assuring that balked landing performance is achievable if on a single engine approach or in the event of engine failure at the landing decision point. Decision height was assumed to be 200 ft, which also supported the use of desirable deceleration schedules of 0.7 to 1 kt/s as mentioned above. The resulting RASCAL specific noise-abatement approach profile is shown in figure 2(c).

## Flight Test Matrix

A total of 8 test points ranging from the test point A to test point H, as shown in table 1, were flown in the acoustic tests. The first two test points, A and B (level flight at 80 knots, and 6 deg descending flight at constant airspeed of 80 kt respectively) were flown for the purpose of obtaining data which could be compared with data measured for another helicopter similar to the RASCAL. These two test points were flown such that the helicopter passed at an altitude of 250 ft over the center microphone (ref. 6). The remaining 6 test points (C through H) were flown at a higher altitude of 400 ft ; this is conducted in according with the ICAO and FAA noise certification practices (ref. 8), and for the purpose of providing a flight database consistent with previous FAA/industry tests with a number of helicopters (refs. 9–11).

In addition to the three noise-abatement approach profiles (i.e., test points F, G, and H) discussed above, three standard descending approaches (9 deg decelerating, 6 deg decelerating, and 6 deg constant speed at 80 knots corresponding respectively to test points D, E, and C) were also flown. These additional test points were designed to permit an assessment of the effects of decelerating approach flight and flying single- and multi-segment approach profiles on the noise characteristics and the associated tracking performance. The deceleraton level of the two single-segment approach profiles, D and E, was also set at the value of around 0.7 to 1 kt/s. Test points C, D, and E were flown in a traditional manner by intercepting the desired flightpath from below the extended glideslope and at specified initial speeds (100 kt for 6 deg, and 65 kt for 9 deg). The set up of the flight experiment is discussed next.

## Flight Experiment Setup

The acoustic tests were conducted at Crows Landing Airfield, Calif. in January 1995. Figure 7 shows the plan view of the facility and the general arrangement of the flight experiment. The helicopter final approach flight track is along the centerline of Runway 35 passing over the two center microphones (the ground board microphone #2 and the tripod stand microphone #3) of the array of 4 microphones. The helipad was located near the "STOL aim point," which was made "movable" to achieve the scheduled flyover altitude of 400 ft above the center microphone #2 for each of the 6 main approaches (test points C to H). For the other two test points, A and B, the scheduled flyover altitude was 250 ft above the center microphone #2. A precision laser tracker, near the "NASA complex," which houses the control room of the experiment, was used to assess the navigational accuracy of the LDGPS. The ground station of the LDGPS was located on the roof of a NASA complex building. Also shown in the figure is the location of the weather balloon of the weather measurement system, which was set up near the Crows Landing Airfield tower on the east side of Runway 35. The implementation of the RASCAL flight systems and the set up of the acoustic/weather measurement systems are described below.

### Navigation, Guidance, and Cockpit Displays

The implementation of the noise-abatement approach guidance in the RASCAL helicopter (ref. 12) has been described in detail in reference 2. Only a brief description is provided here.

The approach profiles shown in table 1 and figure 2(a)–2(c) were formatted in look-up tables and were implemented in the RASCAL's 486-based on-board research computer. Range to the helipad was used as input to the look-up tables, and the height of the desired approach glidepath and the corresponding speed were determined. The range to the helipad information, as well as other aircraft position and

velocity signals, was obtained from transforming the LDGPS navigation data in Earth-Centered-Earth-Fixed coordinates (ref. 13) to a Cartesian coordinate system with origin at the helipad. Errors from the desired references were then calculated, scaled, and transmitted to the existing electromechanical flight instruments of the RASCAL helicopter, figure 8, which was equipped with a three-cue flight director system normally used for conventional ILS approaches.

To adapt these RASCAL displays to noise-abatement approaches, some minor modifications were made to the existing system. The LDGPS guidance commands were formatted in a special interface unit as if they were ILS course deviation signals transmitted over the ILS test frequency. They were made available to the ILS receiver of the RASCAL through a T junction to the ILS antenna cable. With this implementation, the raw data glideslope and localizer display sensitivities were able to be set as desired. Display sensitivities are important parameters affecting handling qualities associated with flying these approaches. For this acoustic flight test, the sensitivity for the glideslope display was of a "linear" type (instead of the conventional angular type), and was set at 25 ft/dot at all ranges. For localizer display, the values of the sensitivity were 88 ft/dot out to the 2000 ft from the helipad. Beyond that range, an angular sensitivity of 1.25 deg/dot was used.

For the three-cue flight director of the RASCAL that was used for these tests, lateral course guidance was realized using the roll steering bar, speed control with the pitch steering bar, and vertical path control with the collective command cue (see fig. 8). Unfortunately, it was not possible to modify the flight director command laws. The collective flight director, which had been originally designed for a constant-speed approach, was found to be less than desirable and was not used in this flight test; as a result, the tests were flown using only a two-cue flight director.

Finally, it is important to briefly describe some current flight control features of the RASCAL helicopter, since it, along with flight displays, affects the handling qualities and the tracking performance, which are discussed later in the paper. The basic UH-60 helicopter is equipped with a rate damping stability augmentation system in pitch, roll, and yaw, with turn coordination capability implemented via limited authority electrohydraulic series actuators. Additionally, parallel electromechanical actuators provided both trim centering and outer loop stabilization. Below 60 knots, the outer loop stabilization included attitude and heading hold features; above 60 knots, it consisted of turn coordination and airspeed stabilization. A trim release switch and a trim beep switch were available for the pilot to change the reference condition or to relieve control forces.

### Flight Test Instrumentation and Data Acquisition and Reduction

Extensive flight data were gathered during the tests, including those from an inertial navigational unit (INU), airdata, cockpit controls and servo actuator displacements, LDGPS, laser tracker, and a newly developed laser-based rotor state measurement system on board the aircraft. The rotor state measurement system (ref. 14) consists of three laser distance transducers mounted on each hub arm of the main rotor, and four linear accelerometers mounted near the root of each blade. Measured data from this system were collected at a rate of 263 Hz, which corresponded to one sample for approximately every 5.88 deg increment in the azimuth angle of the RASCAL main rotor system. This system thus provided a robust measurement and accurate estimation of the space orientation of the rotor tip-path-plane, among other blade motion variables. The tip-path-plane measurements, along with the aircraft attitude and flightpath, permitted an accurate estimation of tip-path-plane angle of attack, which is an important parameter for understanding and correlation of the BVI acoustic data obtained from the wind tunnel with those from flight. This will be further elaborated in the paper later.

### Accoustic and Weather Measurement Systems

For the requirements of this experiment, an array of four microphones was used. This array consisted of two microphones located on the flight track centerline and one each at the starboard and port sidelines located at 500 ft from the center mics. The array was linear and perpendicular to the flight track centerline (see fig. 7). Except for the #3 center mic, which was on a 1.2 meter tripod, each of the remaining three mics (#1, #2, and #4) was placed on a 42 in. $\times$ 42 in. $\times$ 1/2 in. PVC ground board. This was done so that in addition to obtaining acoustic data for the special flight procedures associated with this test, the data could be added to the extensive database associated with reference 6. Additionally, these data would permit researchers to be able to compare EPNL noise footprints as determined from a 3 microphone array to EPNL contours generated from different combinations of microphones used to collect the reference 6 data. The spacing on the four microphone array was that used in the standard ICAO/FAA noise certification test (ref. 8). The microphones were 1/2 in. diameter condenser type fitted with grid caps covered by commercially available foam wind screens.

The acoustic data were recorded on four data channels of a battery operated commercially available digital tape recorder. A separate time channel was used to record a time signal synchronized to the helicopter flight track position time. Each microphone was calibrated with a 124 dB tone at 250 Hz and with a constant amplitude white noise before and after data collection. Acoustic data were recorded at a sample rate of 24,000 samples a second to permit the achievement of a maximum 10 kHz bandwidth. For subsequent BVI noise analyses, the acoustic data signals were reduced to overall sound pressure levels typically associated with the bandwidth of frequencies of the blade vortex interaction noise. This overall BVISPL consisted of an integration of the sound pressures within the frequency band limits of 0.5 to 3 kHz (the 3rd through 46th harmonics of the main rotor blade passage frequency, ref. 6). Data reduction also consisted of obtaining a set of five noise metrics compatible with the helicopter noise database generated by the FAA and industry (refs. 9–11). Three of the metrics are obtained from only the instantaneous sound pressure levels, i.e., overall SPL, dBAmax, and the maximum tone-corrected perceived noise level (PNLTmax). The remaining two metrics, SEL (sound exposure level) and EPNL (effective perceived noise level) are time duration corrected single-event metrics. Additionally, as part of the data reduction for the analysis of each flight, the OASPL, dBA, and PNLT were graphically studied as a function of time and horizontal distance along the flight track to each microphone.

A tethered-balloon weather-measurement system was used to collect barometric pressure, dry and wet bulb temperatures, relative humidity, wind speed and direction over the altitude range of interest. The balloon was located approximately 2500 ft to the side of the Runway 35 (see fig. 7). It was permitted to ascend and descend from ground level to an altitude of 1200 ft at a rate of approximately 1 ft/s. The weather data were collected at a rate of 0.1 Hz. The data acquisition began approximately 30 minutes before each flight. wind speeds were closely monitored, so that no acoustic data were acquired when wind speeds exceed 10 knots within the altitude of interest.

## Test Results

The main results of the flight tests are presented below in two categories: flight mechanics data and acoustic data. The reduction of the flight mechanics data was performed at Ames Research Center, and some of the results were later merged with the acoustic data, which were analyzed at Langley Research Center.

### Flight Mechanics Data

From a handling qualities viewpoint, pilot workload and task performance are important ingredients in assessing the pilot acceptability of flying the multi-segment, noise-abatement, decelerating approach profiles. This aspect of the issue related to the feasibility of achieving noise abatement through the use of specific flight procedures has been addressed previously in some detail in reference 2. Here, other aspects of the issue, which are related to noise-certification flight procedures, effects of decelerating approach flight on BVI noise, and the importance of measuring, in flight, the tip-path-plane angle of attack of the main rotor will now be discussed.

### Flight Technical Errors

The tracking performance was found to be generally within the flight performance window required for noise certification testing. Figures 9(a)–9(c) show some examples of repeated runs of the 6 deg decelerating approaches at 80 knots, Quiet, and HAI-Light approaches. These flight trajectories are plotted as altitude vs. horizontal distance from the helipad. It is seen that the altitude tracking errors are somewhat better for the 6 deg decelerating approaches than for the other two set of approaches. Nevertheless, they are all within the performance window called for in noise certification, i.e., ±30 ft (ref. 8). This can be seen from figures 10(a) and 10(b), which show the mean and standard deviation of all the approaches from run #4 to #23 for two windows. Window 1, shown in figure 10(a), covers the horizontal range of ±1000 ft from the center mics, while window 2, shown in figure 10(b), extends the horizontal coverage to ±2000 ft. These ranges, which both extend beyond the 10 dB-down points from the peak noise at the center mics (as will be shown later), were chosen to demonstrate the consistency of the tracking performance. In terms of time duration, these two windows represented approximately 20, and 40 sec of flight time.

### Rate of Descent vs. Airspeed

It is important to examine the rate-of-descent tracking performance, since the design of the noise-abatement approach profiles originated in the plane of rate of descent vs. airspeed. The test results indicate that the rate-of-descent tracking performance was less than desirable as shown in figures 11(a) and 11(b) for two sample noise-abatement approach runs. The rate of descent errors of the four-segment Quiet profile, figure 10(a), were large, especially in the first descent segment. Pilots commented on the difficulty with which this profile was flown with or

without the collective flight director, which had been designed for a constant speed approach as discussed earlier. Use of a properly designed 3-cue flight director system, especially with the third cue collective-commands properly tuned to the flight dynamics of the decelerating approach of the RASCAL helicopter, should improve the rate-of-descent tracking performance.

**Effects of Deceleration on TPP Angle-of-Attack and Effective Glideslope**

Flight measurements of the TPP angle-of-attack are extremely important for two reasons. First, the TPP angle-of-attack can affect greatly the wake geometry of the main rotor. A simple momentum analysis (ref. 15) reveals that the wake skew angle increases, thus flattening the wake, as the angle of attack increases as shown in figure 12. A consequence of the flattened wake is to potentially decrease the miss distance of the blade when passing the vortices shed by preceding blades, thus conducive to an increased BVI noise. For the gross weight range that was flown, 12,606–14,310 lb, the values of Ct were in the range of approximately 0.0045 to 0.0051 ($Ct/\sigma = 0.055$ to 0.062). For that range of Ct, the wake would be flattened at a rate of almost 1 deg per deg increase in angle of attack at airspeeds above 45 knots for the test helicopter. Another potential effect of the flattened wake due to an increased TPP angle-of-attack is on the directivity of the BVI noise. BVI noise usually exhibits a highly directional radiation pattern, with its major lobe being forward and normal to the blade at the interaction position, which typically occurs in the first quadrant. The flattened wake can therefore potentially move further back in the first quadrant, shifting the BVI lobe more to the starboard side of the rotor. This phenomenon has been observed previously in wind-tunnel tests (ref. 4). In addition to the TPP angle-of-attack, obviously the advance ratio and the thrust coefficient are the other important parameters affecting the wake skew angle as is clear from figure 12.

The second significance of in-flight measurements of TPP is that acoustic tests conducted in wind tunnels (e.g., refs. 3–5) typically measured the TPP angle-of-attack through shaft-tilt angle. This is done by adjusting cyclic pitch so that the TPP is parallel to the hub plane of the rotor. Therefore, TPP angle-of-attack can be controlled and measured precisely in a wind tunnel. By varying the TPP angle-of-attack in this way, simulations for a descent, an ascent, or a level flight condition can be achieved in the wind-tunnel. This key parameter, along with advance ratio, and Ct (or $Ct/\sigma$) constitute a set of parameters that were related to gathered acoustic data in the wind-tunnel. Unfortunately, TPP angle-of-attack cannot be controlled at well in flight, and heretofore it has not been measured accurately to permit a serious effort of correlating acoustic data from flight tests with those measured in wind tunnels.

The TPP angle-of-attack plots were generated for all the approach-flight runs using the RASCAL's laser-based rotor state measurement system described earlier. A sample of two runs is shown in the upper portion of figures 13(a) and 13(b), respectively for 6 deg descent at the constant speed of 80 kts (run #4) and 6 deg decelerating descending flight (run #9). The abscissa of these figures represents the horizontal distance from the helipad. The lower part of these figures shows the quasi-steady flightpath angle and effective flightpath angle, which is elaborated below. The TPP angle-of-attack plots were obtained by first transforming the flapping measurements of the laser transducers in a rotating coordinate system to a non-rotating coordinate using the multiblade coordinate transformation (refs. 14 and 16). The results yielded, among other parameters, the sine and cosine components, $\beta_{1s}$, $\beta_{1c}$, of the blade flapping in the nonrotating system. The TPP angle-of-attack, $\alpha_{TPP}$, was then calculated using the following equations:

$$\alpha = \theta - \gamma_{s.s.} \tag{3}$$

$$\alpha_{TPP} = \alpha - \beta_{1c} - i_s \tag{4}$$

where

$\gamma_{s.s.}$ quasi-steady flightpath angle (deg)

$\theta$ aircraft pitch attitude (deg)

$i_s$ inherent shaft tilt angle (–3 deg)

$\alpha$ aircraft angle-of-attack (deg)

The calculation neglected the effects due to small sideslip and winds during the controlled acoustic tests.

The effective glidepath angle, $\alpha_{eff}$, which accounts for the decelerating effect (ref. 17) was calculated using:

$$\gamma_{eff} = \sin^{-1}\left[\sin\gamma_{s.s.} + \frac{\dot{V}}{g}\right] \tag{5}$$

The acceleration along the flightpath, $\dot{V}$, was calculated approximately by a numerical differentiation of the airspeed with respect to time, assuming calm air conditions. The airspeed was first appropriately conditioned with a 0.2 Hz low pass filter. The quality of the approximation has not been assessed with the calculations using the INU or LDGPS derived data.

The results are plotted in the lower part of figure 13 showing the effect of deceleration. As the aircraft decelerated (see also fig. 14, with its abscissa now being shown in airspeed for the 6 deg decelerating approach of

fig. 13(b)), the TPP angle-of-attack increased significantly. The value of the TPP angle-of-attack was generally between the effective flightpath angle and the quasi-steady flightpath angle. Most of the increase in the TPP angle-of-attack during deceleration was due to an increase in aircraft pitch attitude (see fig. 15), with an accompany smaller increase in TPP tilt back with respect to the rotor shaft, to generate the desired level of approximately 0.05 g of deceleration. The result was a significant increase in the effective rate of descent, as seen from the rotor, as indicated in figure 16.

For the three multi-segment noise-abatement profiles, the TPP angle-of-attack values were again seen to lie between the quasi-steady flightpath angle and the effective flightpath angle, which included the effect of deceleration. This is shown in figure 17. Within the critical range of 1000 ft of horizontal distance from the center mics, the TPP angle-of-attack increased and exceeded 10 deg for the HAI-Light run #22. The resultant effective rate of descent of approximately 1500 fpm was reached for the run in the airspeed range of 50–60 knots when flying over the microphones, as can be seen in figure 18. For the Quiet approach run #14, figure 18(a), the effective rate of descent, when flying over the center mics, was increased from the scheduled 500 fpm, which was based on quasi-steady considerations, to some 800 fpm due to the effect of deceleration. Similarly, significant increases in the rate of descent were seen for the HAI-Medium run, figure 18(b), when deceleration effect was included.

It is important, therefore, to point out that the design of decelerating approach profiles based on acoustic data obtained solely from a matrix of various constant slope, constant airspeed quasi-steady approach tests, conducted in a wind tunnel or in full-scale flights, is inadequate to achieve the desired goal of noise abatement. Deceleration effects must be considered. Deceleration alters the TPP angle-of-attack of the main rotor(s), which, as discussed previously, can result in significant changes in the BVI noise characteristics of the helicopter.

It is also worth mentioning that deceleration is usually favorable if descending below the BVI intensive region (called “fried egg”), as in the HAI’s Fly Neighborly Guide. Although the HAI guide also suggests an alternative path of flying above the fried egg, deceleration can increase the effective descending rate, thus leading to an intrusion into the BVI intensive region. This alternative flightpath is therefore less favorable.

### Flight Accoustic Data

The accoustic data were first processed to generate plots of overall sound pressure level (SPL) and A-weighted SPL as functions of time for each microphone station for each run. A-weighted SPL and PNLT acoustic data as a function of horizontal distance from the center mics at the moment of reception time for mics 1,2, and 4 for each run were also produced. It is to be noted that for all of the data analysis presented in this paper, only the ground board microphone data were considered. Figure 19 shows an example of the dBA vs. distance plots for the groups D (6 deg deceleration), E (9 deg deceleration), F (Quiet), and H (HAI-Light). A study of figure 19 shows that there is an in-group consistency within several dB out to distances of approximately 2500 ft in front of and past the centerline microphone. The critical 10 dB down points were generally within ±1000 ft of the center mics as shown in these figures. This is the reason that the flight technical errors discussed earlier were assessed based on the windows of ±1000 ft and ±2000 ft. As expected, the center microphone registered the highest noise level, since it is considerably closer to the aircraft flight track than the two sideline mics. Also, the directivity effect was evident, with the starboard side being considerably (several dB) noisier than the microphone on the port side.

**Run-to-run dBAmax comparison–** Figure 20 summarizes the dBAmax of all groups tested. The dBAmax of the 6 deg decelerating approaches (group D) turned out to be very close to that of the 9 deg decelerating approaches (group E). Although the average dBAmax at the center mic for the D group was 1.4 dB higher than that for the E group, both the starboard and the port mics registered a slightly smaller value of the average dBAmax, in the amount of 0.7 and 0.5 dB, for the group D than for the group E. Comparing the group C (constant speed approach at 80 knots) with group D, deceleration appeared to reduce the noise level somewhat. The average dBAmax value of the group C was higher than that of group D at all the three mic locations. The average dBAmax of the center mic for group C was 2.2 dB higher than that of group D.

An analysis of the group-to-group dBAmax variation of the three multi-segment noise abatement approach profiles presented in figure 20 was determined to be relatively small, amounting to less than 2.3 dB. It is interesting to note that the in-group variation was relatively large, however, for the HAI-Medium profile (group G) and the HAI-Light profile (group H). The average dBAmax at the center mic #2 and the starboard mic for the HAI-Light profiles was the lowest of the three groups, both being 2.2 dB less than the highest group of the Quiet profile. (For the center microphone, this also amounts to a 2.4 dB reduction from the standard 6 deg decelerating approach profile of the group D.) Interestingly, the directivity effect was strong, particularly for the Quiet profile. For this profile, the average dBA max at the starboard mic

location was more than 7 dB higher than that at the port side mic. As a result, the Quiet profile registered, at the port microphone location, the lowest average dBAmax of all the profiles tested. This can be seen from figure 20.

In addition to dBAmax, other instantaneous sound-level metrics, such as OASPL and PNLTmax (ref. 18) were also calculated from the measured acoustic data and compared for each run tested. The general trends of the PNLTmax values are very similar to those of the dBAmax shown in figure 20. However, for the OASPL, the quiet-to-noisy ranking for the groups changed significantly. At the center mic, the average OASPL value was the lowest for the group of 9 deg decelerating approach profile (group E), followed by 6 deg at 80 knots, 6 deg decelerating, HAI-Medium, Quiet, and HAI-Light. The lowest group E was approximately 6.8 dB of the OASPL below the noisiest group H. For this instantaneous sound-level metric, the directivity effect became less pronounced when compared to dBAmax discussed earlier.

**Run-to-run SEL comparison–** It is important to also assess the noise characteristics using duration corrected single-event metrics to account for added annoyance due to duration. Two metrics, SEL and EPNL, were calculated for all the runs at each mic location. Figure 21 shows a run-to-run comparison for those runs in the groups C through H. The EPNL plots follow the same trend as the SELgraphs in figure 21, but the EPNL dB values are 3 to 4.5 dB higher than the SEL dB values.

The difference in SEL dB values between the 6 deg constant approaches and the 6 deg decelerating approaches was very slight, less than 1 dB for all the mic locations. In this case the improvement with deceleration was very little for this helicopter. With the level of deceleration flown for the 6 deg decelerating approaches, the TPP angle-of-attack increased on the order of about 3 deg (see fig. 13), which would, as seen from the rotor, appear to be flying on a 9 deg glideslope over the centerline mics. At the scheduled flyover airspeed of 66 knots (see table 1), it could not be expected to improve the noise impact over the constant 80 knots 6 deg approaches, based on the acoustic data shown in figure 4. It should be pointed out, however, that the situation would likely be quite different for an HAI-Light or HAI-Medium helicopter having the “fried egg” (area of maximum BVI noise) well within the normal operational approach envelope as shown in the HAI guide (ref. 1). In those cases, deceleration is likely favorable if descending below the fried egg, because deceleration will result in an increased effective descent rate thus moving further away from the BVI noise-intensive region.

As with the dBAmax data discussed earlier, the SEL data for the three ground board microphones (#1, #2, and #4), presented in figure 21, also show a mixed result for the 6 and 9 deg decelerating approaches. A slight improvement is observed for the 9 deg decelerating approaches relative to the 6 deg approaches at the center mic #2, but with a slight degradation at the starboard mic. For the three multi-segment decelerating approach profiles, the average SEL value of the HAI-Light group was again the lowest, some 2.3 dB lower than the highest Quiet group at the center mic. The directivity effect was again very strong as can be seen clearly in figure 21.

**dBAmax and SEL statistics–** The mean, standard deviation, and range of SPL’s established by the minimum and maximum values of the measured acoustic data were also calculated using the five noise metrics for all the groups at each microphone location. Figure 22 shows the plots of the dBAmax and SEL metrics at the centerline microphone #2. The open circles indicate the mean values; the horizontal bars connected with a vertical line indicate the standard deviation and the solid diamond symbols indicate the range. As described earlier, the in-group variation is fairly large, especially for the HAI-Medium group. The standard deviation tends to be smaller for the SEL than for dbBAmax. For the center mic shown, the mean value of dBAmax increased from HAI-Light to HAI-Medium, 9 deg deceleration, Quiet, 6 deg deceleration, to 6 deg at constant 80 knots of airspeed. The range of the mean value was less than 5 dB for the dBAmax and less than 3 dB for SEL.

## Discussion

It is obvious from the experimental results that the Quiet approach profile did not yield the lowest noise of the various profiles tested. This appears reasonable, if one recalls that the profile design was based largely on the acoustic data obtained from steady flight at constant airspeeds and constant glideslopes as shown in figure 4. No deceleration effects were considered in the profile design process, partly because of the lack of experimental data. In decelerating flight, however, the TPP angle-of-attack of the main rotor increases to provide the desired level of deceleration. This can be seen from figures 13, 14, and 17, and was discussed in some detail previously. As a result, the effective rate of descent, as experienced by the main rotor, increases as shown in figures 16 and 18 in the plane of descent rate vs. airspeed. With the nominal increases in the rate of descent, commensurate with the level of deceleration at 0.05 g, properly accounted for and added to figure 4, the result is shown in figure 23. This is a more appropriate basis to realistically evaluate and to gain some understanding of the results of the acoustic data described above.

With the deceleration effect considered, the descent rate of the Quiet profile is now around 800 fpm, instead of the scheduled 500 fpm, at and near the airspeed flying over the mics. The result is to increase significantly the noise impact, as can be seen clearly in figure 23. Also shown in the figure, indicated with the asterisks, are the effective descent rates of the HAI-Medium and HAI-Light profiles at the airspeeds when flying over the microphones. The acoustic data set was not dense enough in the region near the asterisks to permit a reliable estimate; however, when interpolating among the available data, the HAI-Medium and HAI-Light profiles appeared to produce noise impact no worse than the Quiet profile. Similarly, the other three conventional approach profiles tested, i.e., 6 deg at constant speed of 80 knots, 6 deg deceleration, and 9 deg deceleration, can be interpreted with the help of figure 23.

Thus, after taking deceleration effects into account, all three decelerating noise-abatement profiles tested pass through nearly the same region of moderately noisy characteristics of the test helicopter, as the microphone array is crossed. This implies that the test helicopter is a poor candidate for assessing the merit of noise reduction through the use of special approach flight procedures, because it has no clearly defined fried egg plot within the operational approach envelope as is the case for a HAI-Light helicopter, for example.

Another important effect of deceleration is the change to the directivity of the BVI noise. Deceleration increases the TPP angle-of attack, which tends to flatten the rotor wake, thereby shifting BVI positions further back in the first quadrant. The result is a change in directionality of the BVI noise, moving the BVI lobe more to the starboard side. This and other effects discussed earlier are among the main reasons why it is important to provide accurate measurements of the main rotor TPP angle-of-attack in an acoustic flight test. Although there is a potential substitute for the direct measurement of the TPP with the use of the effective flightpath angle described previously, a thorough evaluation must be made on the quality associated with the estimation of the effective flightpath angle. Also, because of the strong BVI directivity, test methods specifically with respect to suitable number of microphones and their locations probably need further developing and improving.

The effect of deceleration in a descending approach flight on the effective rate of descent, has important ramifications on the design of an approach profile. The increase in the rate of descent, commensurate with the level of deceleration, should be included in the design process. A potential application of this requirement is given in figure 24, which shows a HAI recommendation (ref. 1) on two options for conversion to approach flight in order to avoid the BVI intensive region. Based on the above discussions, the preferred path will have to be the lower one as indicated in the figure. Also, a helicopter that has BVI characteristics as shown in figure 24, which exhibits a more focused BVI intensive region and located more within the operational approach envelope than was the case for the test helicopter, figure 4, would offer much more promise for showing significant benefits in using these noise-abatement approach procedures.

## Concluding Remarks

An acoustic flight experiment was conducted using the NASA/Army RASCAL research helicopter with its recently developed LDGPS-based cockpit display capabilities. The flight tests were conducted at Crows Landing Airfield in northern California with an array of four microphones similar to that used in the standard ICAO/FAA noise certification test. A newly developed, laser-based rotor state measurement system on board the aircraft was used to measure the main rotor tip-path-plane angle-of-attack. An assessment of the noise reduction effectiveness and associated tracking performance of a RASCAL-specific BVI noise-abatement approach profile (called Quiet), two HAI-recommended generic noise abatement profiles—one for medium weight and one for light weight helicopters—and three conventional descending approaches, namely, 9 deg decelerating, 6 deg decelerating, and 6 deg constant speed at 80 knots, was made. The results showed that

1. Using LDGPS guidance for positioning over the microphones, the flight technical errors were small, generally within the flight performance window required for the noise certification test.

2. The Quiet approach profile, which was designed using acoustic flight test data appropriate to the test helicopter but without considering the effect of deceleration on the effective descent rate, showed no reduction in BVI noise from the standard 6 deg or 9 deg decelerating approaches.

3. The effect of deceleration on descending approach flight was found, with the help of the newly developed, laser-based rotor-state measurement system installed on the RASCAL helicopter, to increase the tip-path plane angle-of-attack of the main rotor with an accompanying increase in the effective rate of descent. The effect can influence significantly the BVI noise characteristics. The design of a deceleration approach profile for BVI noise abatement should therefore consider the effect of deceleration.

4. At the centerline microphone location, the mean value of dBAmax increased from HAI-Light to HAI-Medium,

9 deg decelerating, Quiet, 6 deg decelerating, to 6 deg at constant speed of 80 knots, with the range being less than 5 dB. Similar ranking was found with the use of SEL noise metric; however, the range was somewhat smaller, being less than 3 dB.

5. The directivity effect of the BVI noise was found to be very strong. The average dBA max of the test runs measured at the starboard microphone location was approximately 6 dB higher than that at the port mic location (about 4.6 dB difference in SEL metric). Deceleration along the approach increased the TPP angle-of-attack, which tended to accentuate the directivity.

## References


1. Anon.: Fly Neighborly Guide. Helicopter Association International, 1992
2. Hindson, W. S.; and Chen, R. T. N.: Flight Tests of Noise Abatement Approaches for Rotorcraft Using Differential GPS Guidance. AHS Annual Forum, May 1995
3. Martin, R. M.; and Connor, A. B.: Wind-Tunnel Acoustic Results of Two Rotor Models with Several Tip Designs. NASA TM-87698, July 1986
4. Liu, S. R.; and Marcolini, M. A.: The Acoustic Results of a United Technologies Scale Model Helicopter Rotor Test at DNW. AHS Annual Forum, May 1990
5. Gallman, J. M.; and Liu, S. R.: Acoustic Characteristics of Advanced Model Rotor Systems. AHS Annual Forum, May 1991
6. Mueller, A. W.; Conner, D. A.; Rutledge, C. K.; and Wilson, M. R.: Full Scale Flight Acoustic Results for the UH-60A Airloads Aircraft. presented at the AHS Vertical Lift Aircraft Conference, San Francisco, Calif., Jan. 1995
7. Wilson, M. R.; Mueller, A. W.; and Rutledge, C. K.: A New Technique for Estimating Ground Footprint Acoustics for Rotorcraft Using Measured Sound Fields. presented at the AHS Vertical Lift Aircraft Conference, San Francisco, Calif., Jan. 1995
8. Leverton, J.: Helicopter Noise Certification, Past-Present-Future. 18th European Rotorcraft Forum, Avignon, France, Sept. 1992
9. Yoshikami, S. A.; and Cox, C. R.: FAA/HAI Helicopter Flight Operations Noise Tests and Initial Results. AHS Annual Forum, May 1985
10. Yoshikami, S.A.: Flight Operations Noise Tests of Eight Helicopters. FAA-EE-85-7, Aug. 1985
11. Rickley, E. J.; Jones, K. E.; Keller, A. S.; and Fleming, G. G.: Noise Measurement Flight Test of Five Light Helicopters. DOT/FAA-EE-93-01, July 1993
12. Jacobsen, R. A.; Rediess, N. A.; Hindson, W. S.; Aiken, E. W.; and Bivens, C. C.: Current and Planned Capabilities of the NASA/Army Rotorcraft Aircrew Systems Concepts Airborne Laboratory (RASCAL). AHS Annual Forum, May 1995
13. Kaufmann, D. N.: Helicopter Approach Capability Using the Differential Global Positioning System. NASA CR-177618, Aug. 1993
14. Fletcher, J. W.; Chen, R. T. N.; and Strasilla, E.: State Estimation of Main Rotor Flap and Lead-Lag Using Accelerometers and Laser Transducers on the RASCAL Helicopter. submitted for presentation at 34th AIAA Aerospace Science Meeting, Reno, Calif., Jan. 1996
15. Chen, R. T. N.: A Survey of Nonuniform Inflow Models for Rotorcraft Flight Dynamics and Control Applications. NASA TM-102219, Nov. 1989
16. Chen, R. T. N.: Effect of Primary Rotor Parameters on Flapping Dynamics. NASA TP-1431, Jan. 1980
17. Hoh, R. H.; Baillie, S. W.; and Traybar, J. J.: Determination of Decision Height Windows for Decelerating IMC Approaches in Helicopters. AGARD Conference Proceeding 508, Feb. 1991
18. Bennett, R. L.; and Pearsons, K. S.: Handbook of Aircraft Noise Metrics. NASA CR-3406, 1981

Table 1. RASCAL/LDGPS noise-abatement acoustic tests approach flight profiles tested

| Test PT | Flight conditions | Airspeed over mic | Run # |
|---|---|---|---|
| NASA 748 comparison | | | |
| A | 250 ft level flight @ 80 kts | 80 kt | 1, 2, 3 |
| B | Descent 6 deg @ 80 kts (250 ft over center mic) | 80 kt | 4, 5, 6, 23 |
| RASCAL/LDGPS acoustics | | | |
| C | Descent 6 deg @ 80 kts (400 ft over center mic) | 80 kt | 7, 8 |
| D | 6 deg decelerating ( “) | 66 kt | 9, 10 |
| E | 9 deg decelerating ( “) | 54 kt | 11, 12 |
| F | Quiet critter (“) - multisegment, decel | 63 kt | 13, 14, 15 |
| G | HAI Medium ( “) - multisegment, decel | 50 kt | 16, 17, 18, 19 |
| H | HAI Light ( “) - multisegment, decel | 54 kt | 20, 21, 22 |

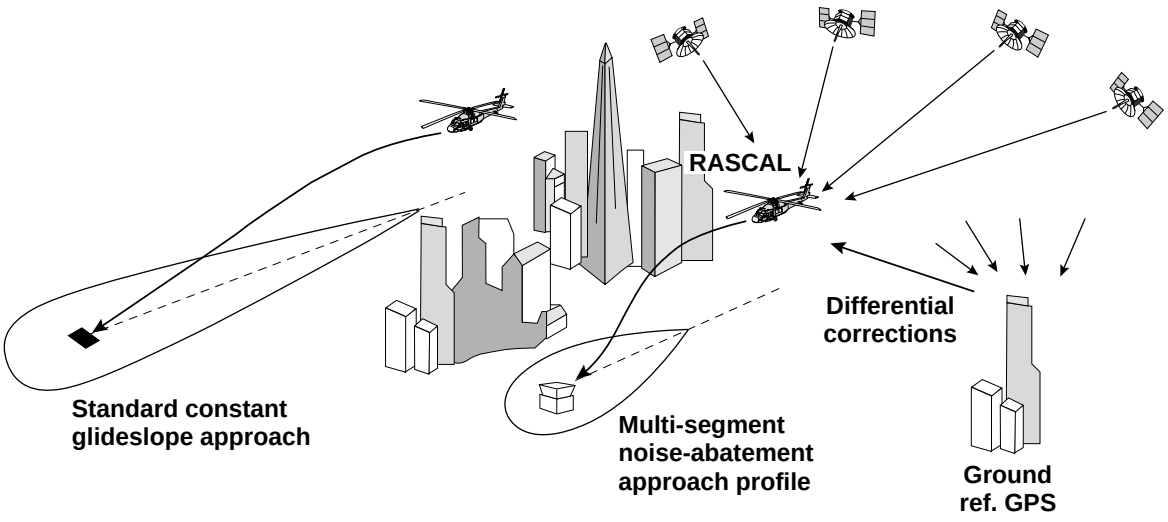


*Figure 1. Schematical diagram showing LDGPS-guided rotorcraft noise-abatement approaches in a confined urban area.*

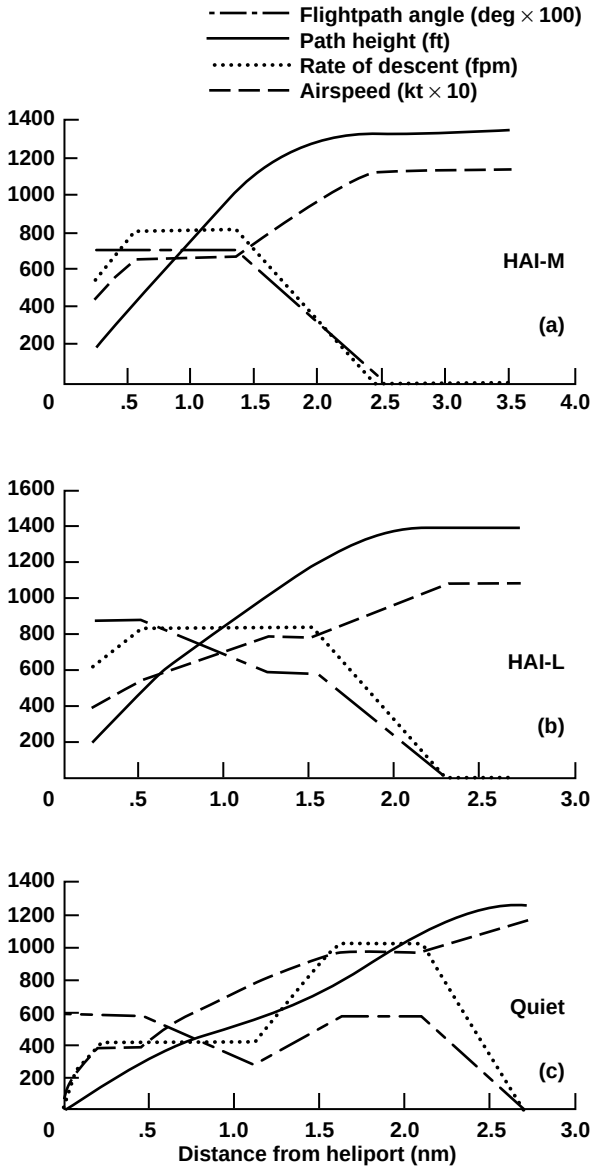


*Figure 2. Approach profile details: (a) HAI-Medium, (b) HAI-Light, (c) Quiet.*

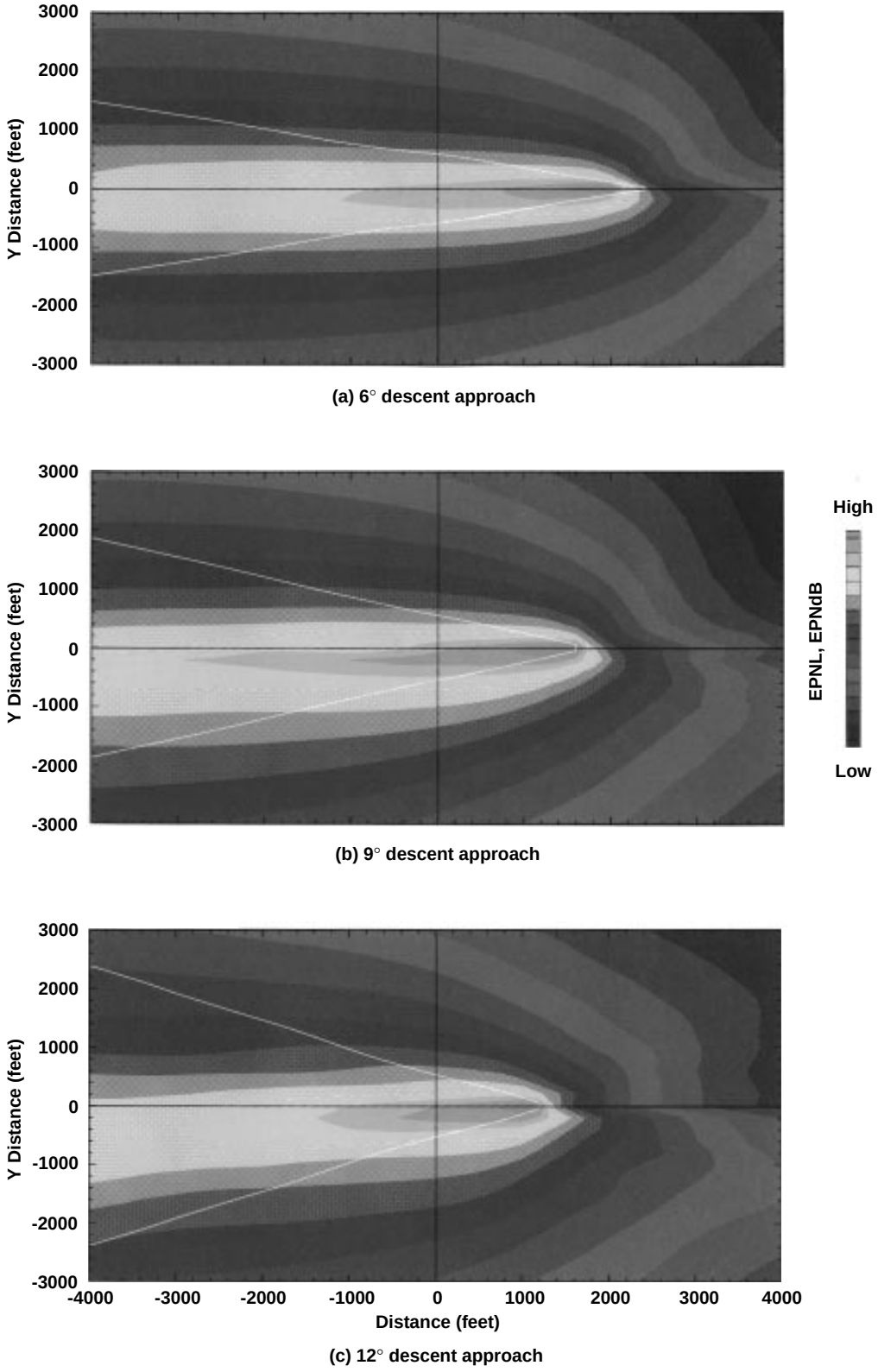


*(a), (b), (c) Varying glideslope @ 80 kts*

*Figure 3. EPNL ground footprints in descent flight.*

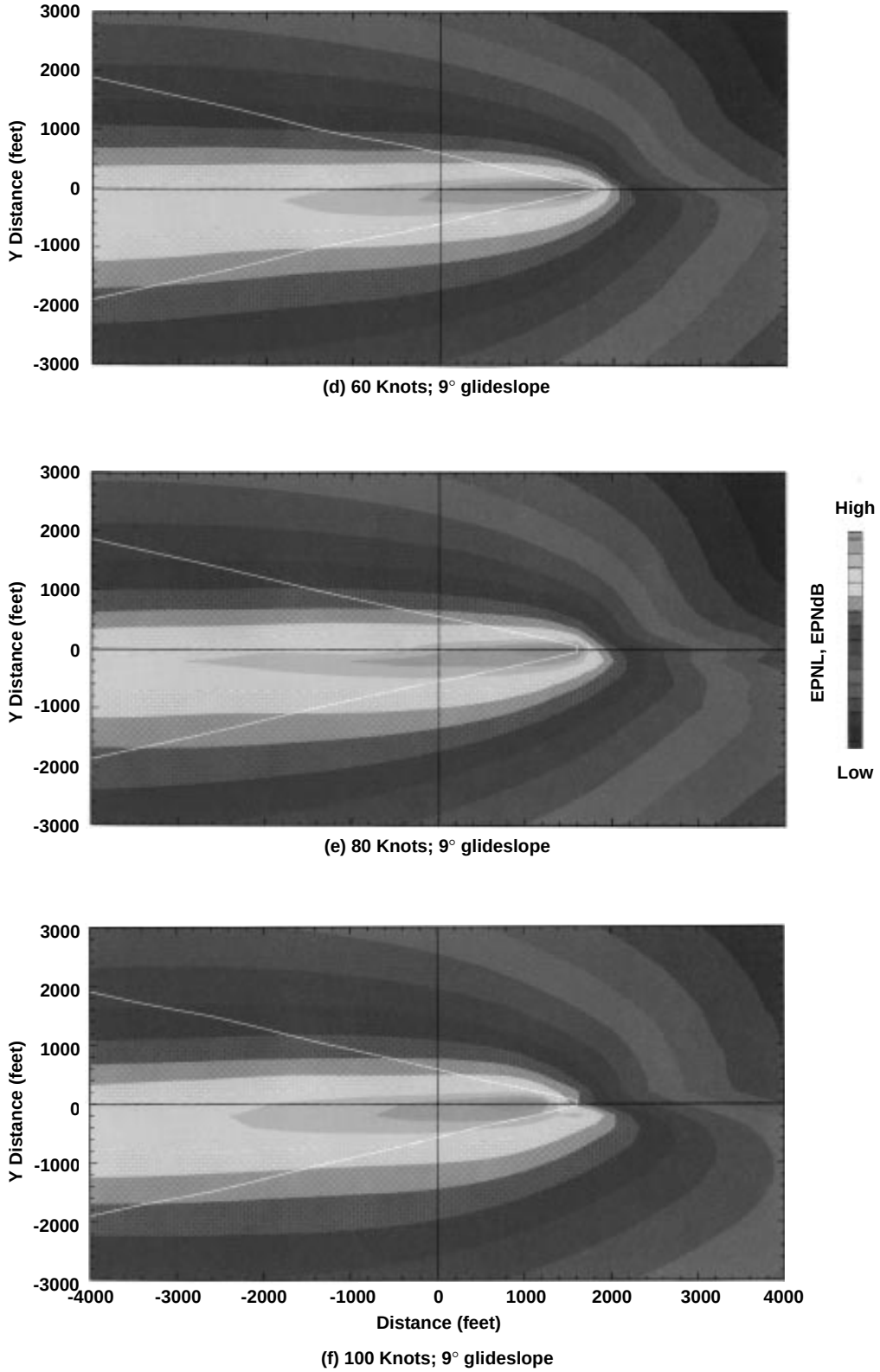


*(d), (e), (f) @ 9 deg glideslope with different constant speeds*

*Figure 3. Concluded.*

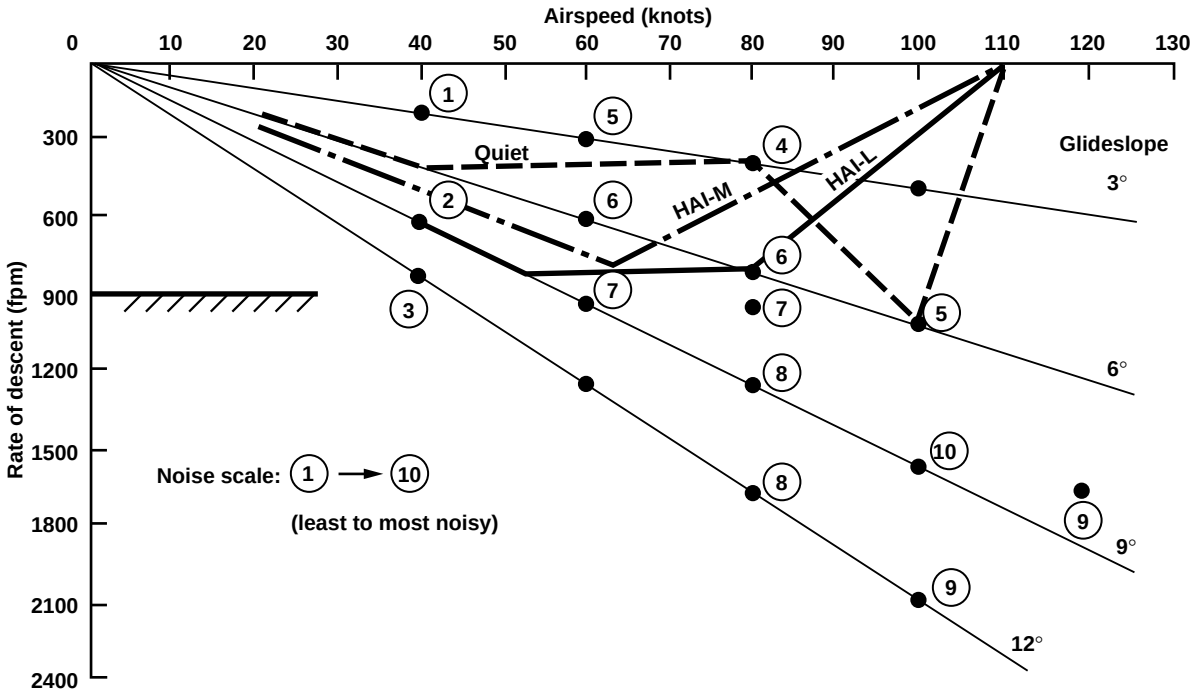


*Figure 4. Tested noise-abatement approach profiles in the plane of airspeed vs. rate of descent.*

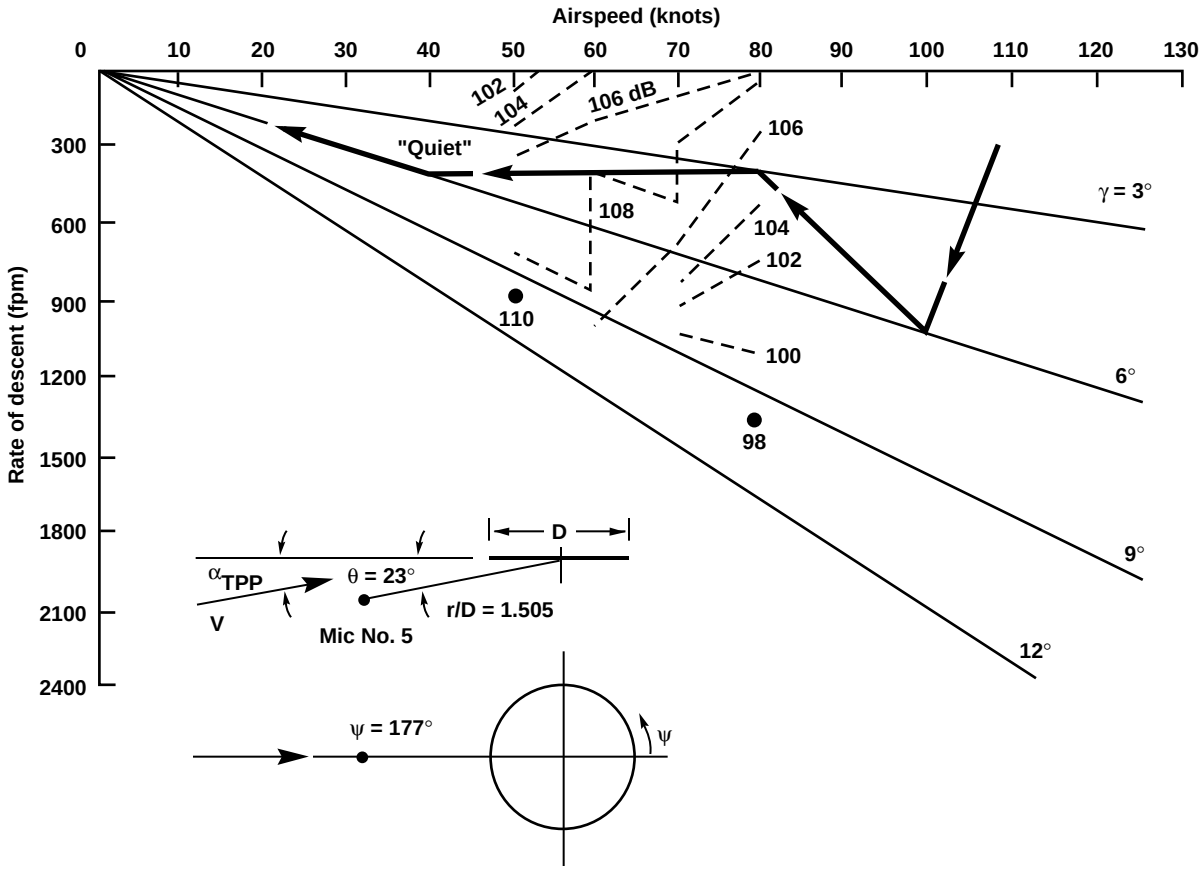


*(a) Center mic (#5)*

*Figure 5. BVI noise in descent – Langley 14- by 22-Foot Subsonic Wind Tunnel data.*

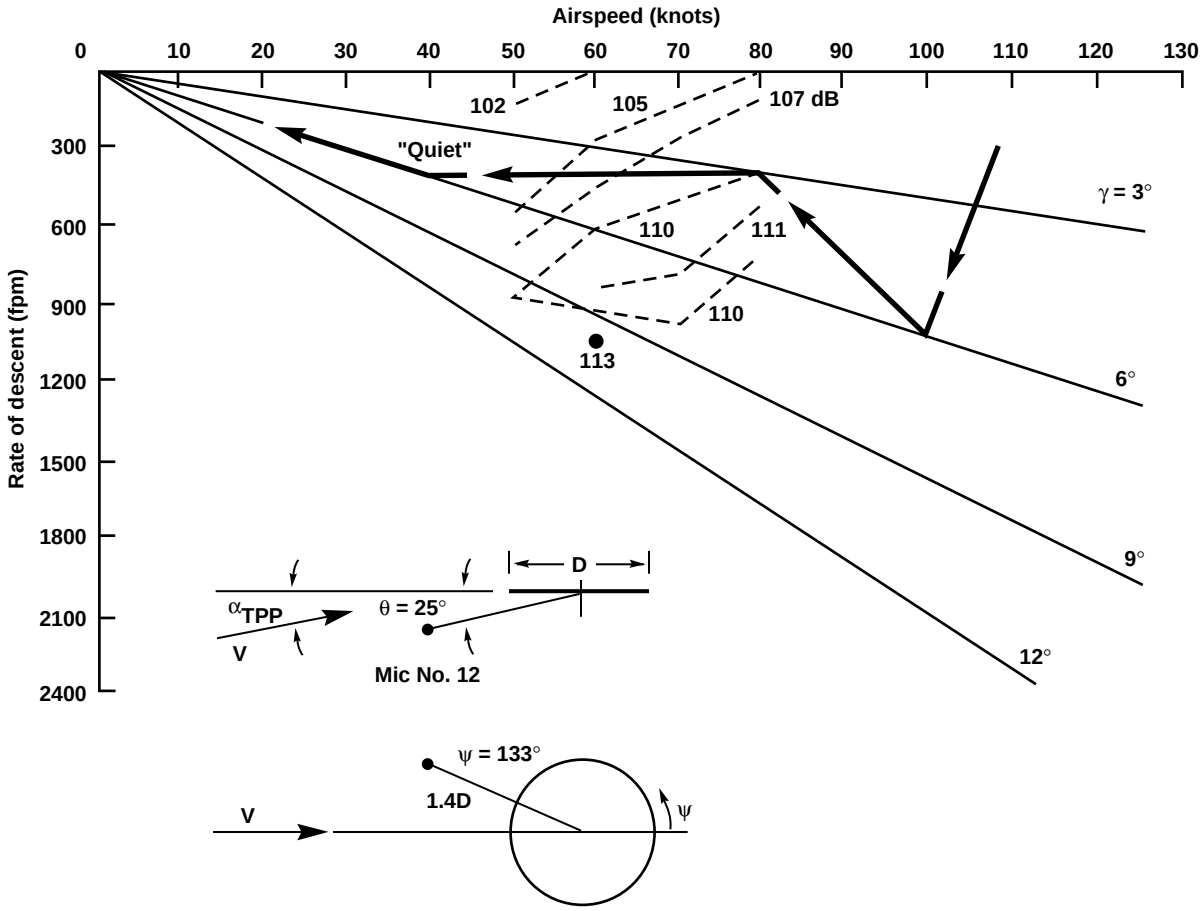


*(b) Starboard mic (#12)*

*Figure 5. Concluded.*

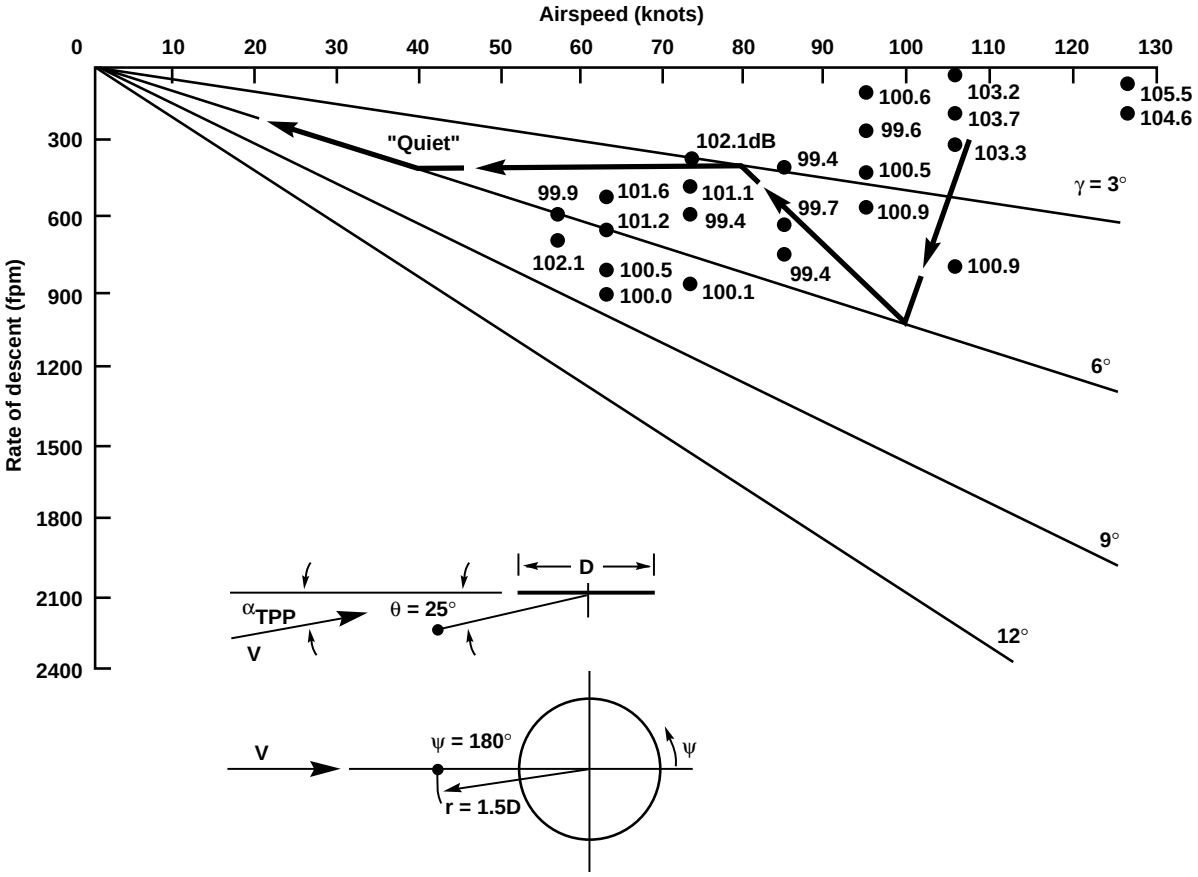


*(a) Center mic (#3)*

*Figure 6. BVI noise in descent – DNW tunnel data.*

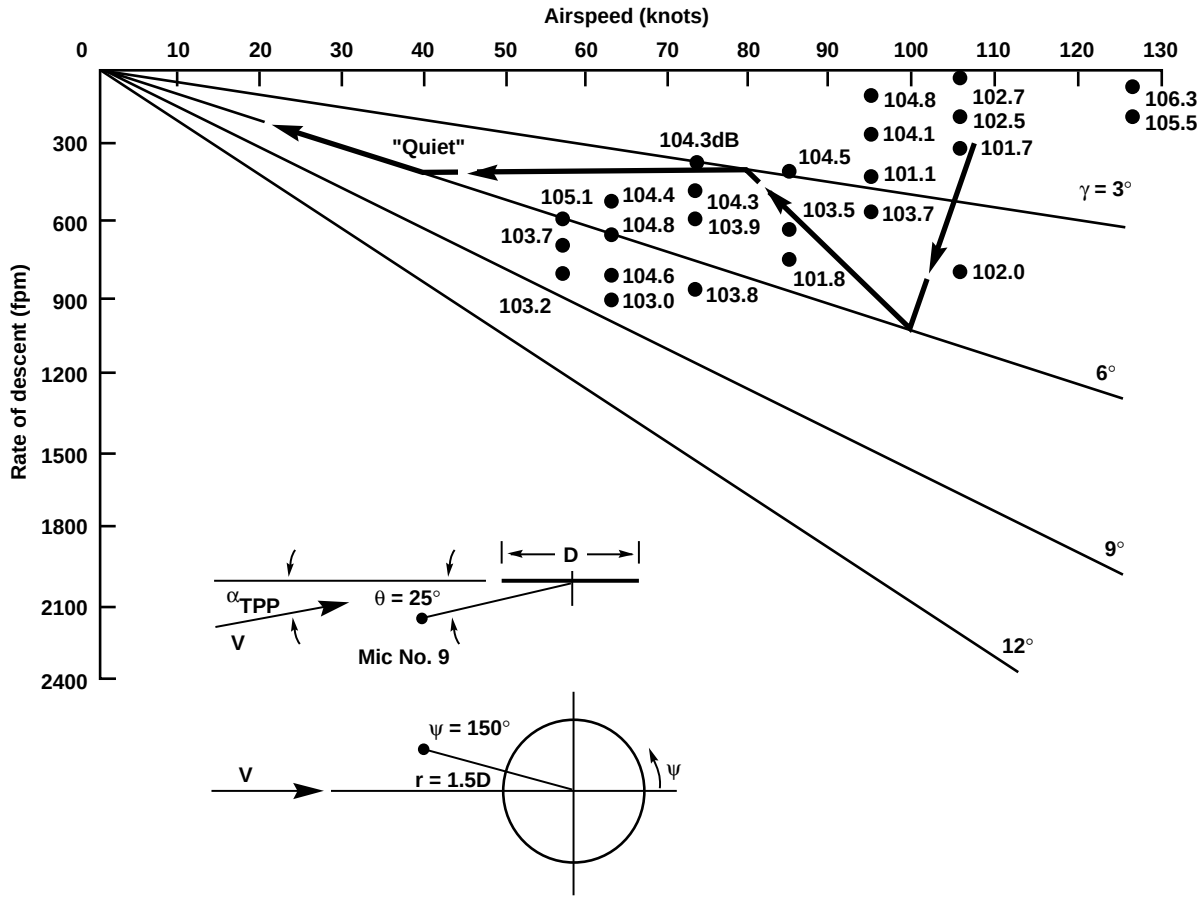


*(b) Starboard mic (#9)*

*Figure 6. Continued.*

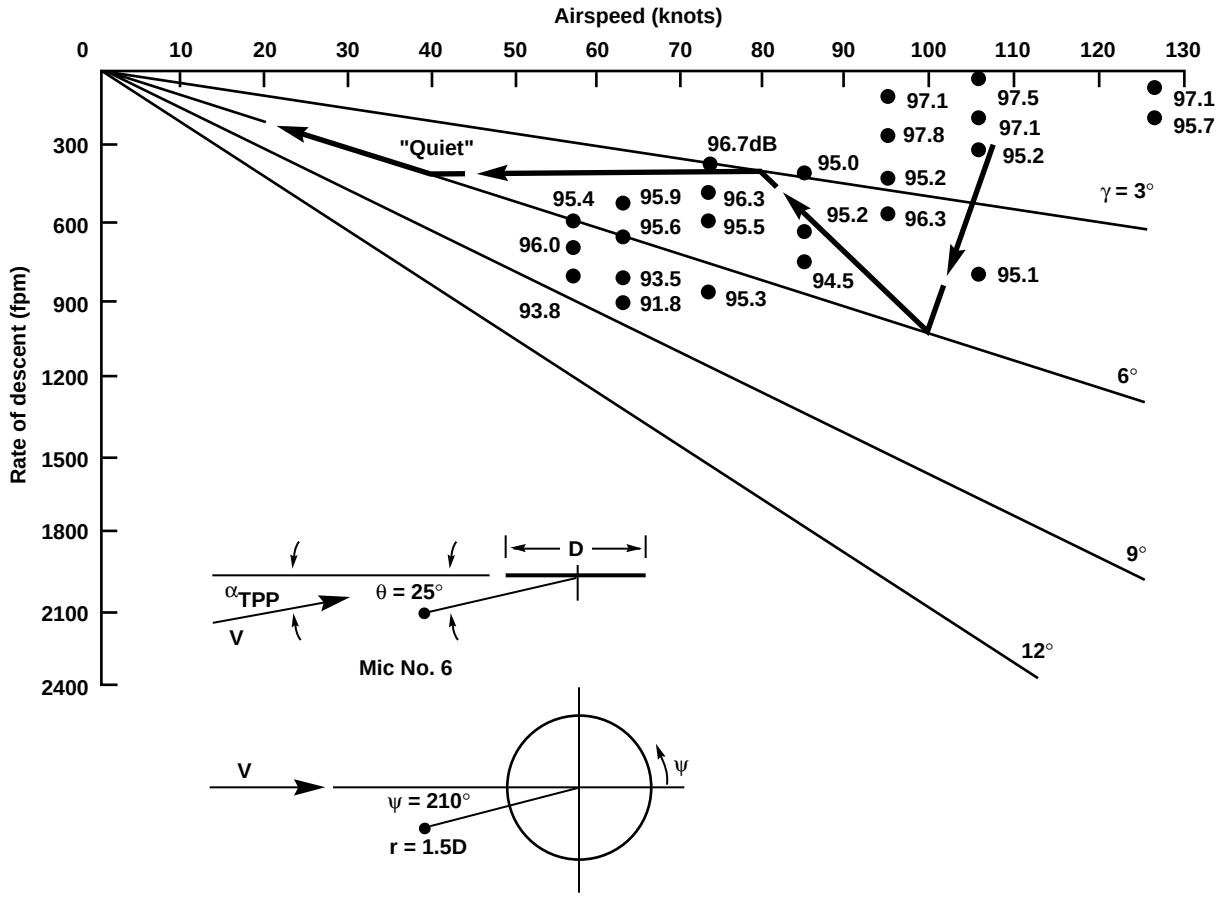


*(c) Port mic (#6)*

*Figure 6. Concluded.*

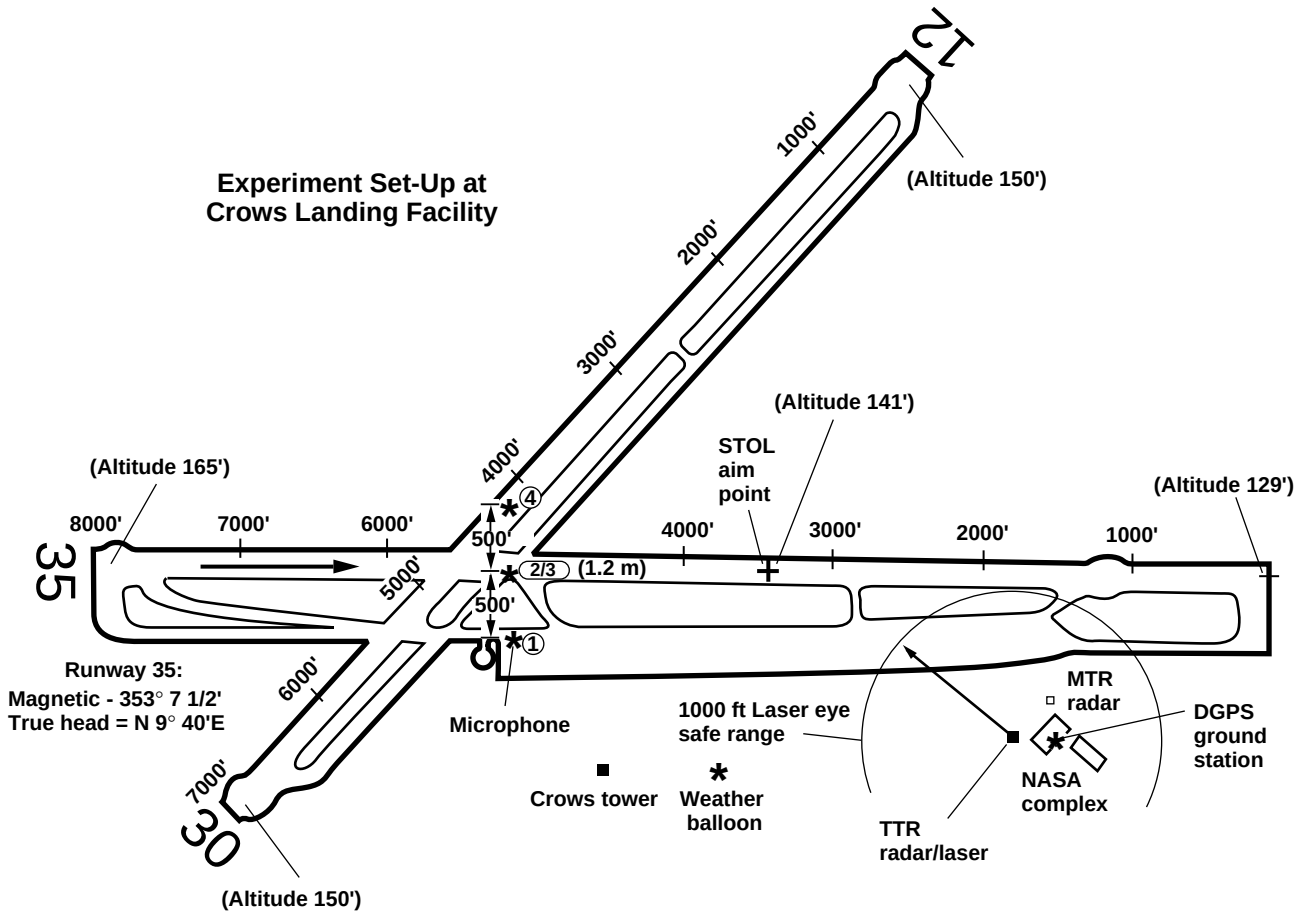


*Figure 7. Experiment set-up at the Crows Landing Facility.*

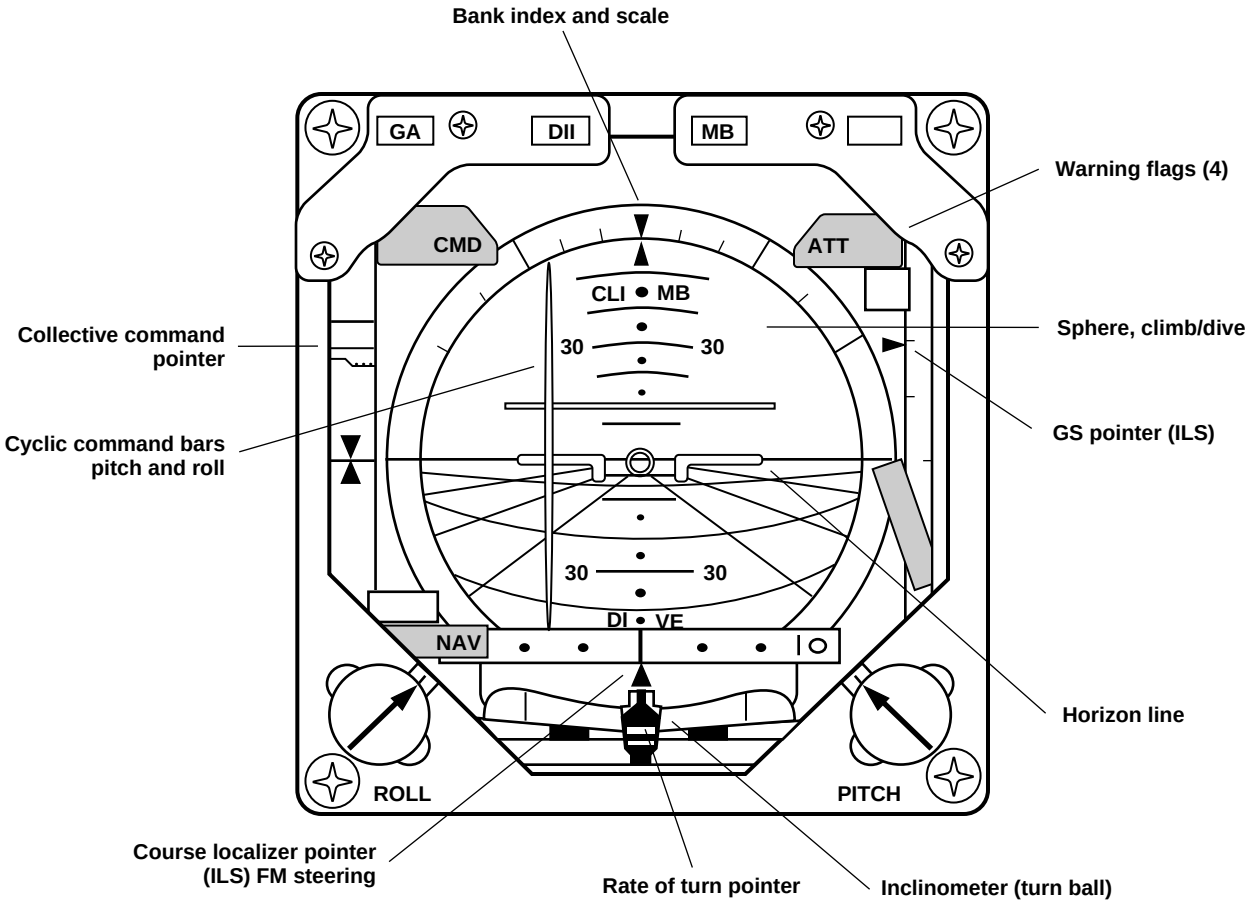


*Figure 8. Vertical situation indicator and flight director display.*

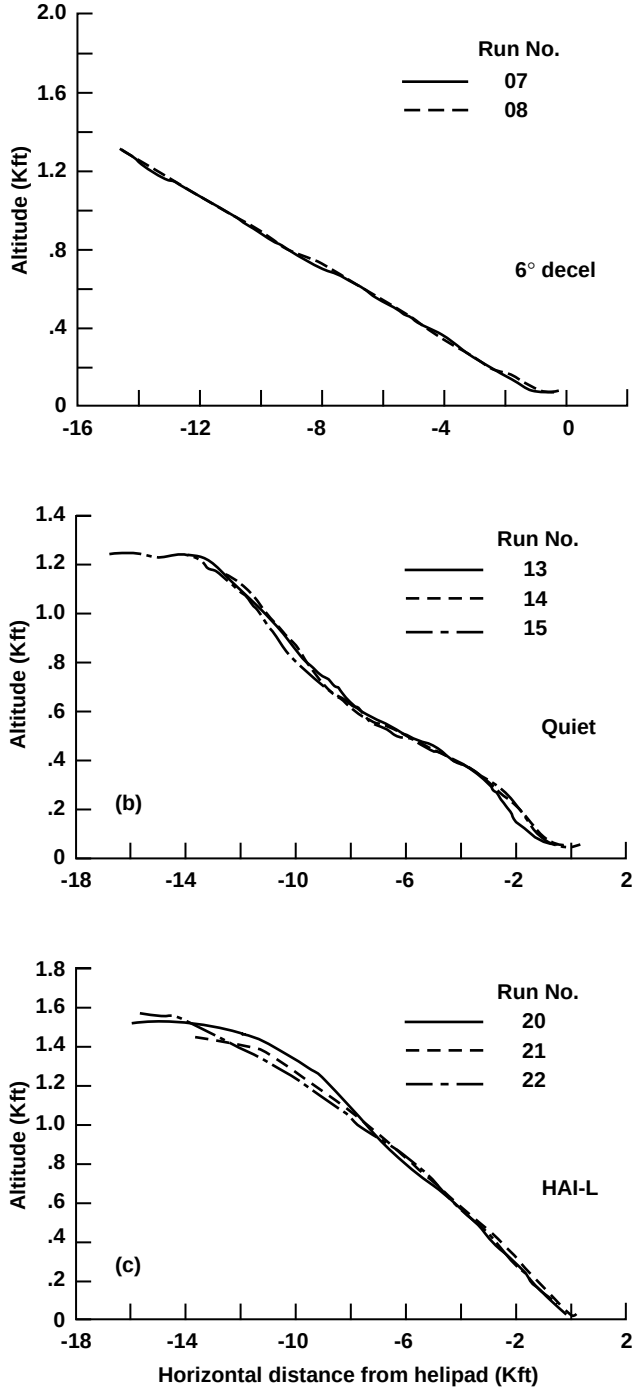


*Figure 9. Flight trajectories of some repeated runs. (a) 6 deg decel., (b) Quiet, (c) HAI-Light.*

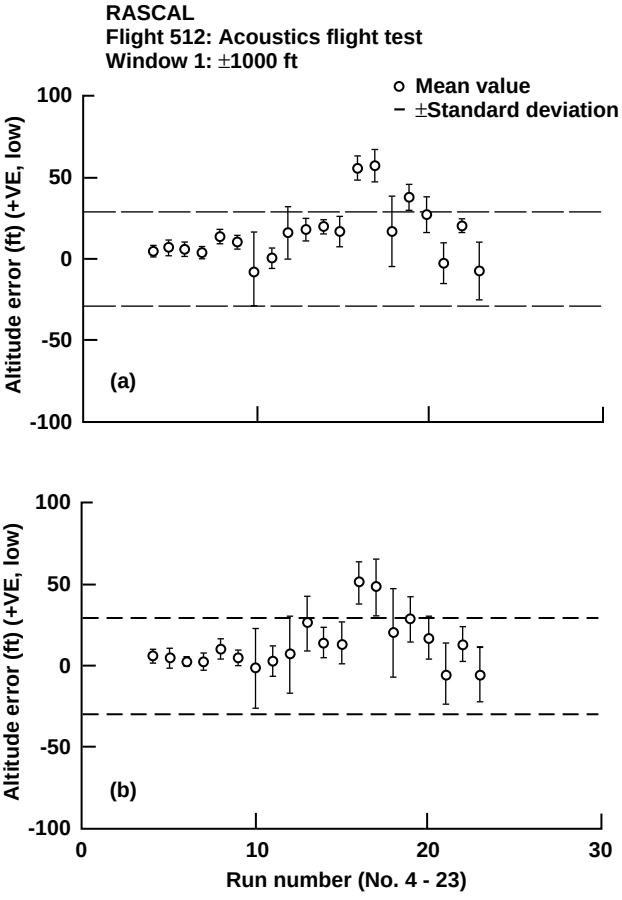


*Figure 10. Flight altitude errors of runs #4 to #23 for two windows. (a) window 1 – ±1000 ft in horizontal distance from center mic #2, (b) window 2 – ±2000 ft.*

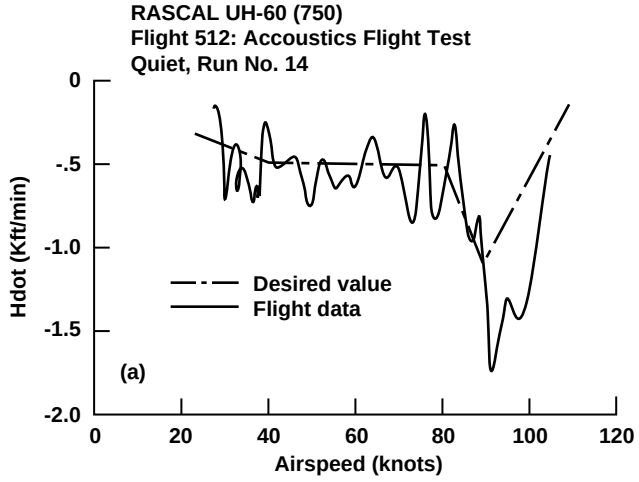


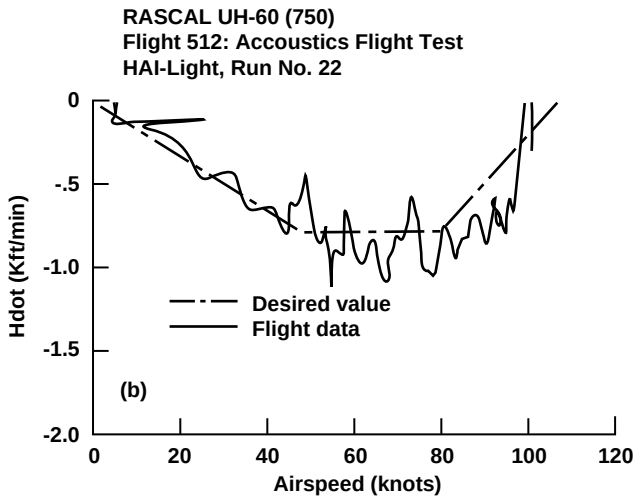


*Figure 11. Example of rate of descent tracking performance. (a) Quiet run #14, (b) HAI-Light run #22.*

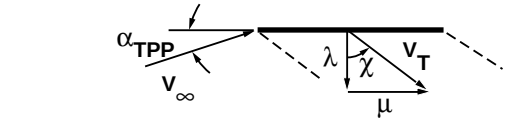


**Wake skew angle:**

$$\tan\chi = \frac{\mu}{\lambda}\ ;\ \mu = \frac{V_\infty \cos\alpha}{\Omega R}\ ;\ \lambda = v_o - \frac{V_\infty \sin\alpha}{\Omega R}$$

**(a)**

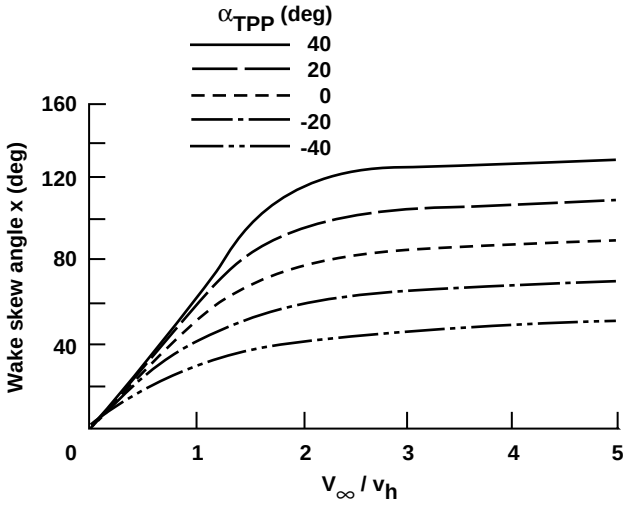


**(b)**

*Figure 12. Effect of tip-path-plane angle-of-attack on wake skew angle. (a) definition of wake skew angle, (b) effects of TPP angle-of-attack, Ct, and advance ratio on wake skew angle.*

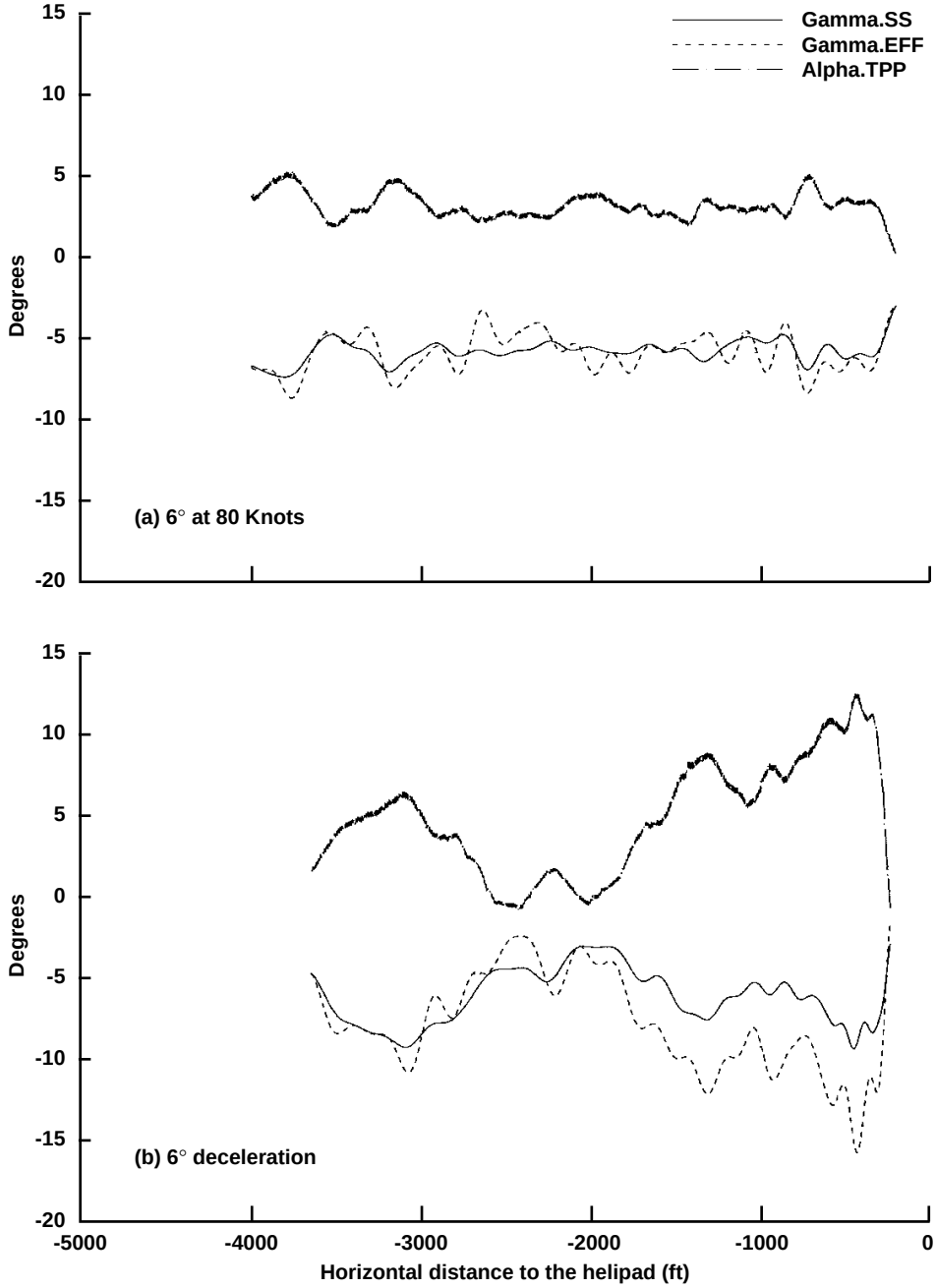


*Figure 13. Sample plots of TPP angle-of-attack, steady-state and effective flightpath angles vs. horizontal distance to the helipad. (a) 6 deg descent @ 80 kts, (b) 6 deg decelerating descent flight.*

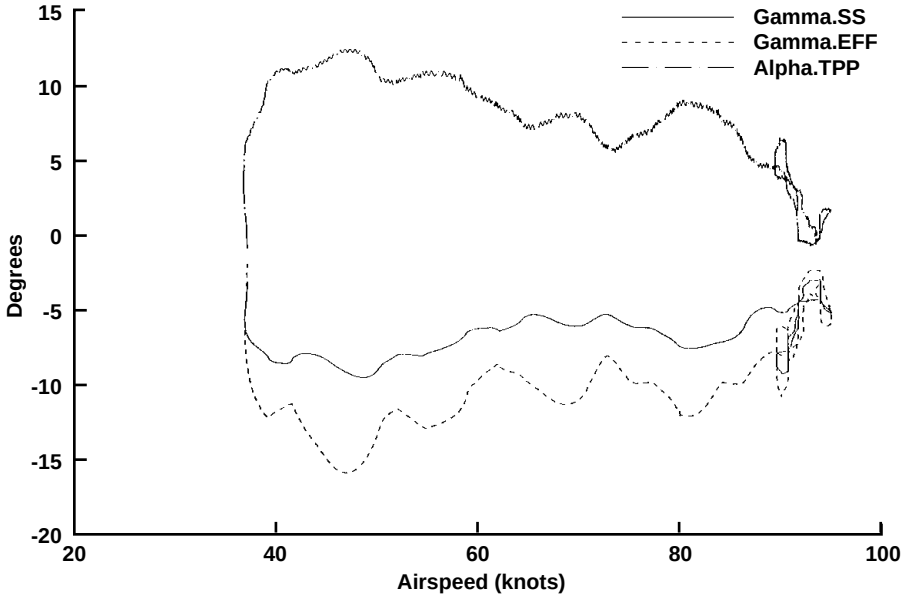


*Figure 14. TPP angle-of attack, steady-state and effective flightpath angles vs. airspeed plots for a 6 deg decelerating descending flight (run #9).*

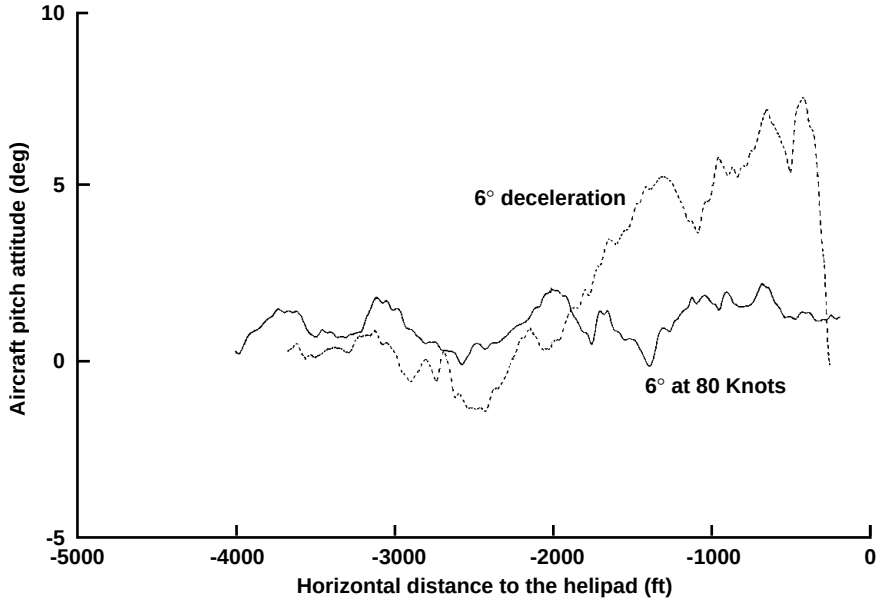


*Figure 15. Aircraft pitch attitude vs. horizontal distance-to-the helipad plot for a 6 deg decelerating descending flight (run #9).*

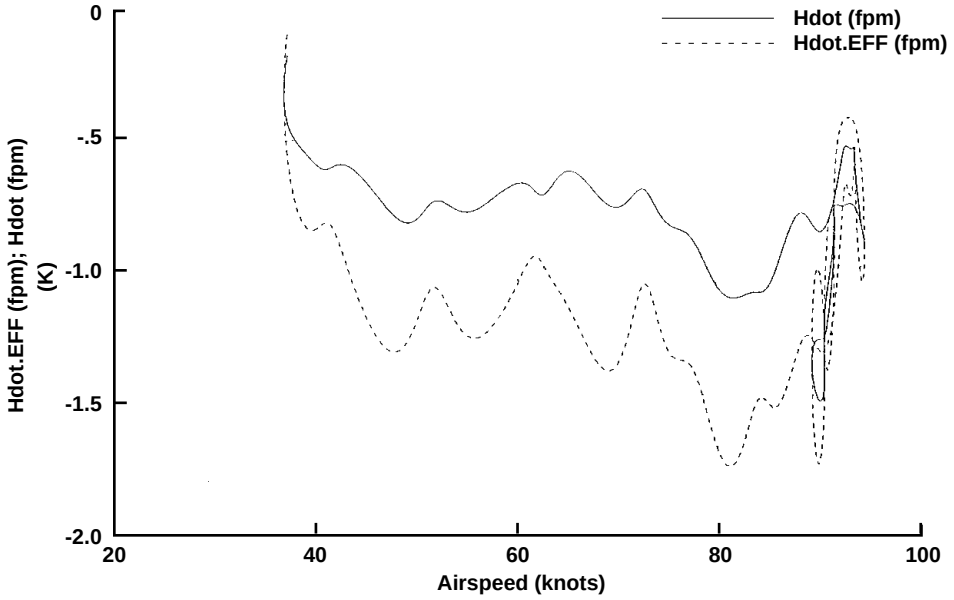


*Figure 16. Quasi-steady and effective rate of descent vs. airspeed plots for a 6 deg decelerating descending flight (run #9).*

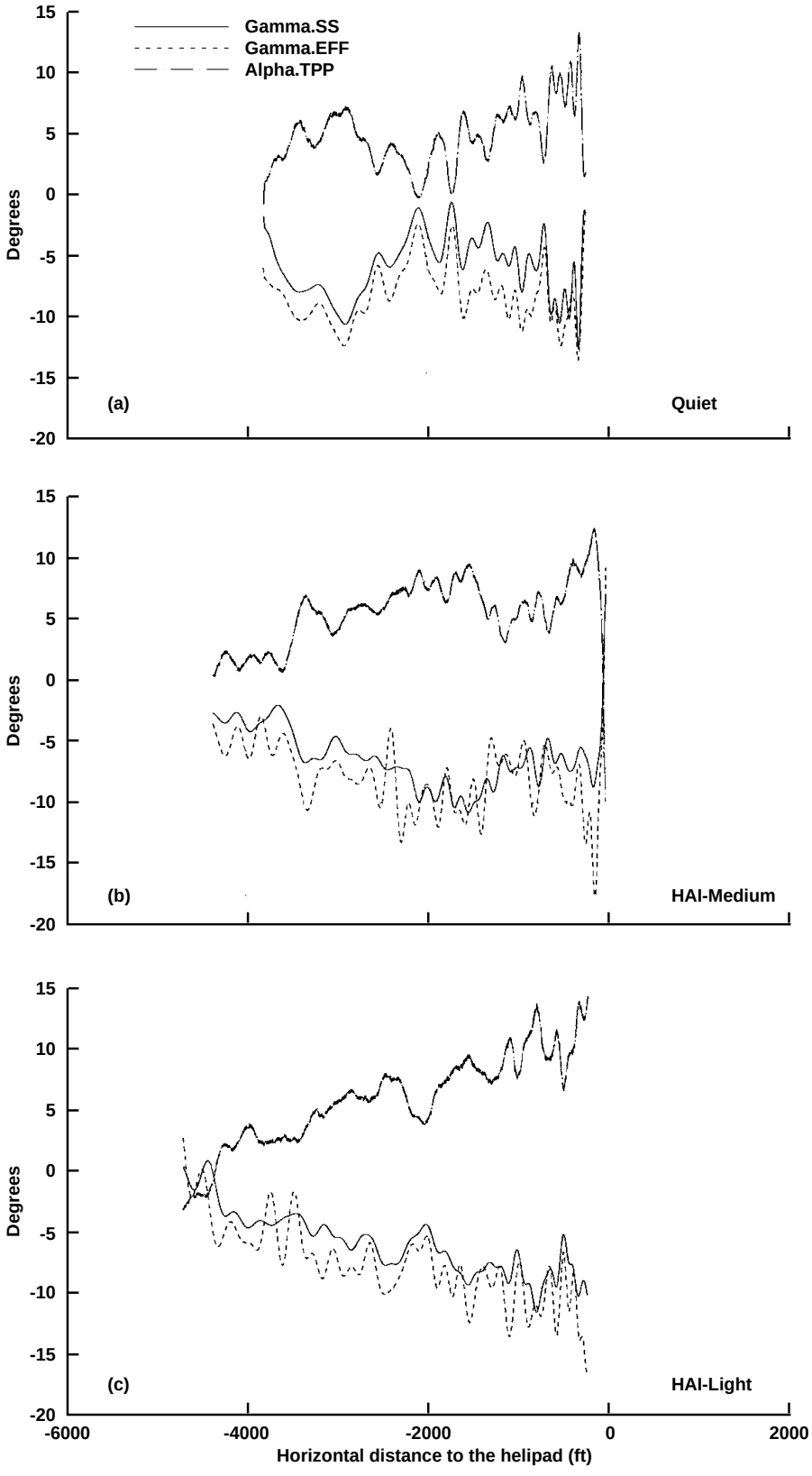


*Figure 17. Sample plots of TPP angle-of-attack, steady-state and effective flightpath angles vs, horizontal distance to the helipad. (a) Quiet, (b) HAI-Medium, (c) HAI-Light.*

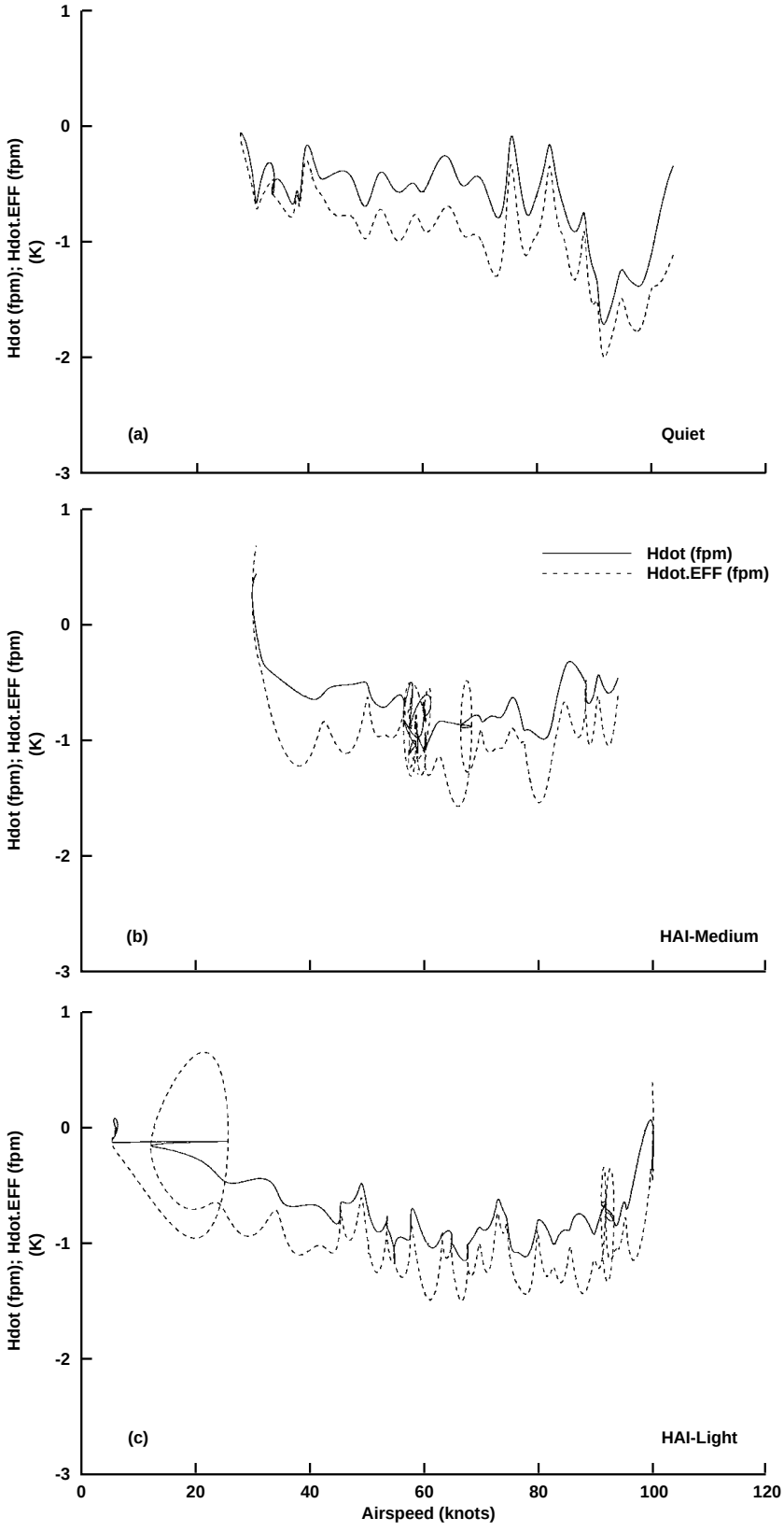


*Figure 18. Quasi-steady and effective rate of descent vs. airspeed plots for sample runs of (a) Quiet, (b) HAI-Medium, (c) HAI-Light.*

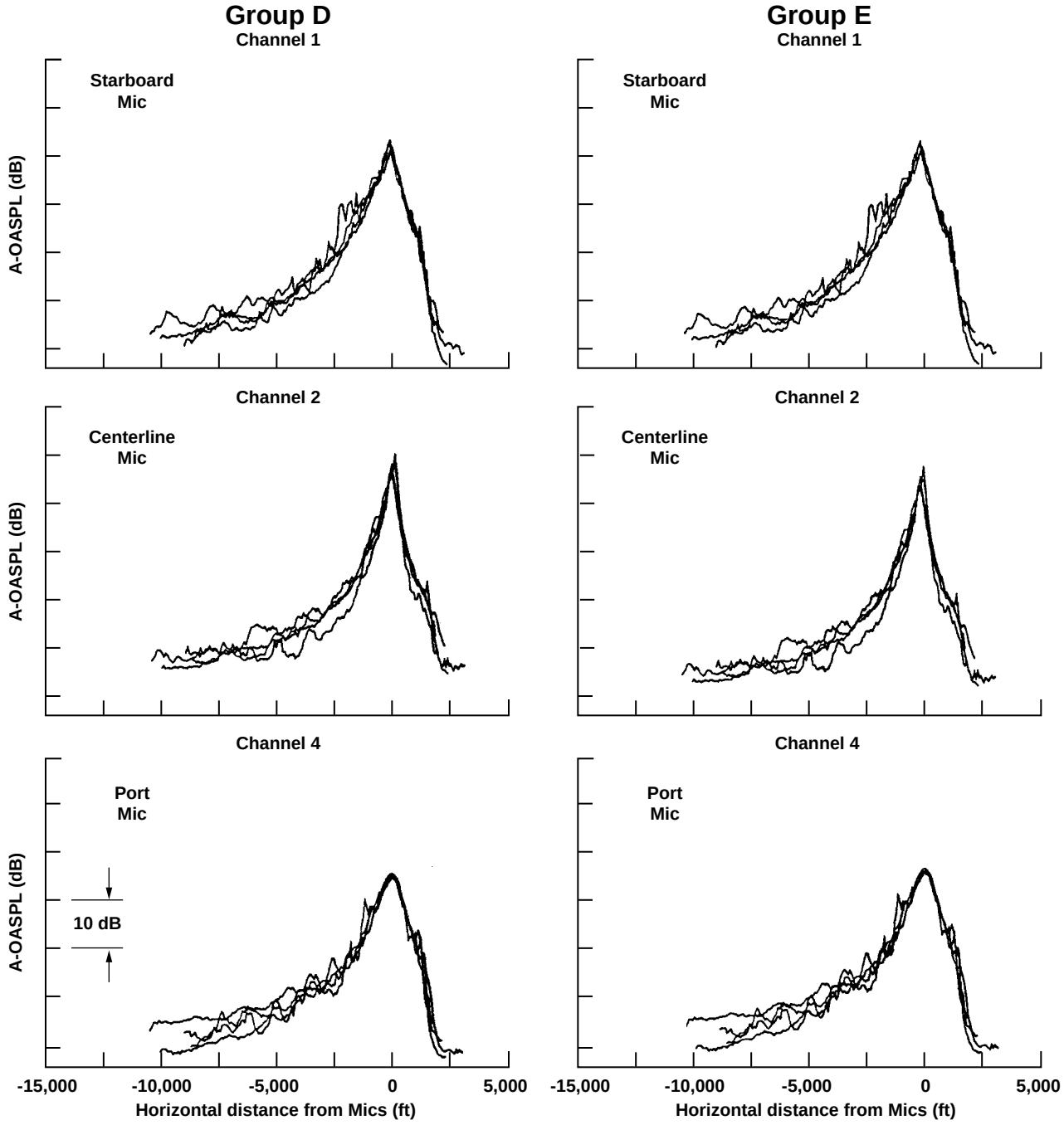


*Groups D (6 deg deceleration) and E (9 deg deceleration)*

*Figure 19. dBA vs. horizontal distance-to-the-center mics plots (all plots with the same scale).*

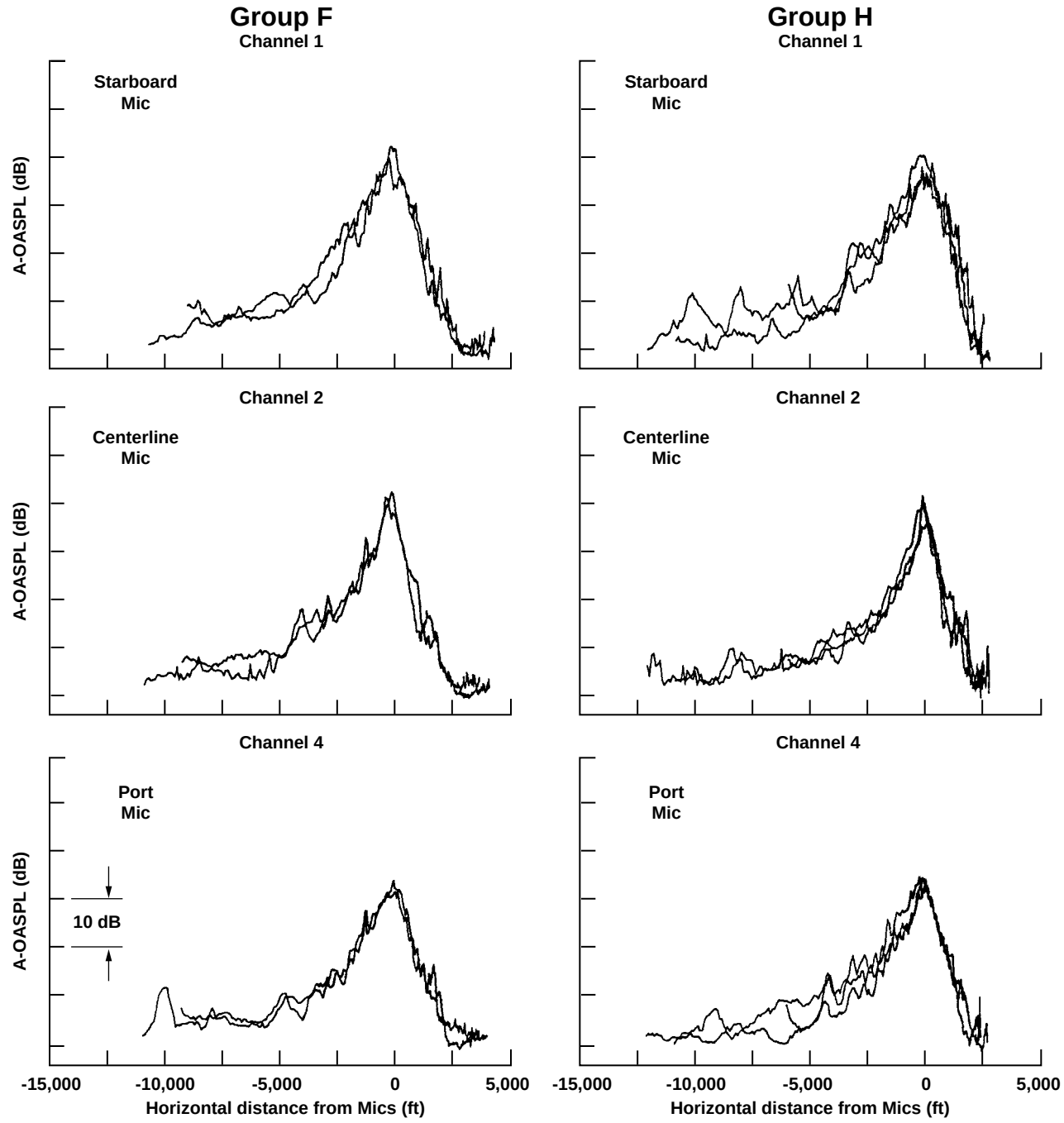


*Groups F (Quiet) and H (HAI-Light)*

*Figure 19. Concluded.*

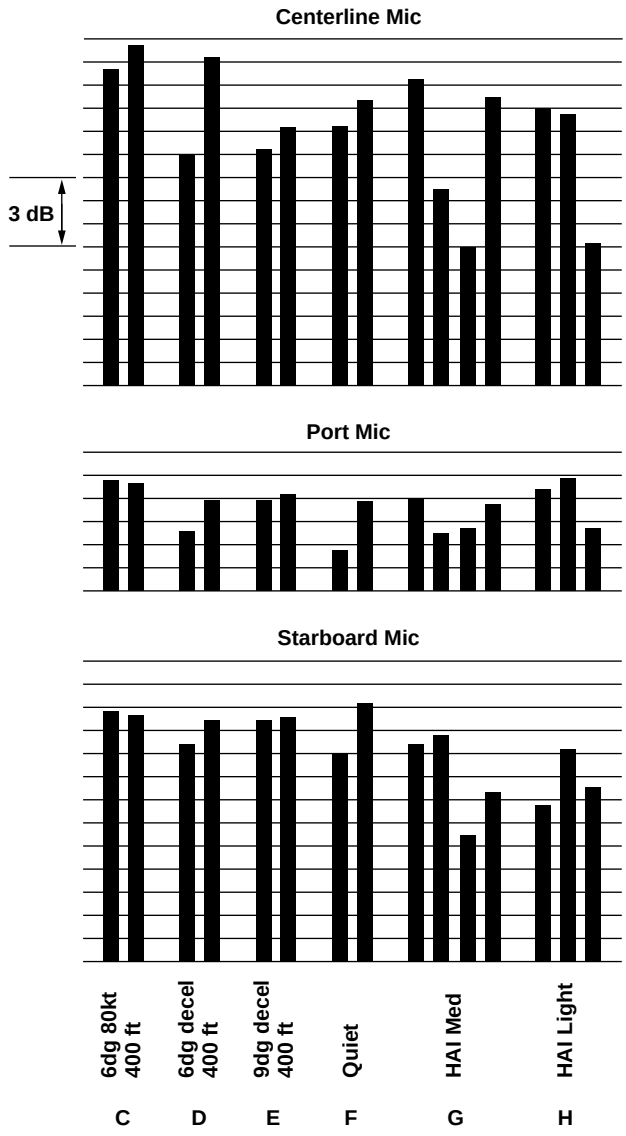


*Figure 20. dBAmax comparsion for groups C (6 deg @ 80 kts), D (6 deg deceleration), E (9 deg deceleration), F (Quiet), G (HAI-Medium), and H (HAI-Light) at the three mic locations. (Note: The baselines and the scales are the same.)*

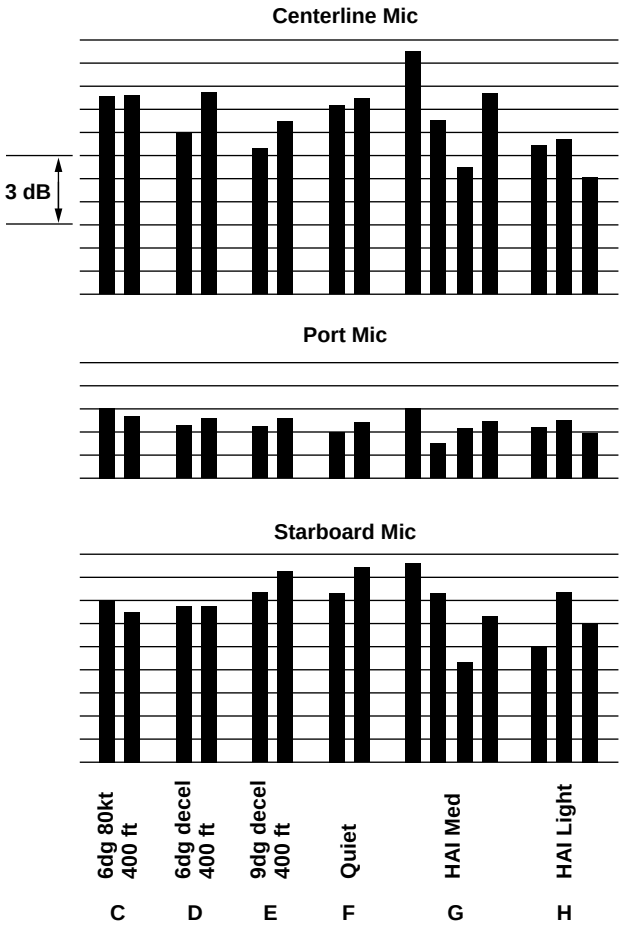


*Figure 21. SEL dB comparison for groups C (6 deg @ 80 kts), D (6 deg deceleration), E (9 deg deceleration), F (Quiet), G (HAI-Medium), and H (HAI-Light) at the three mic locations. (Note: The baselines are and the scales are the same.)*

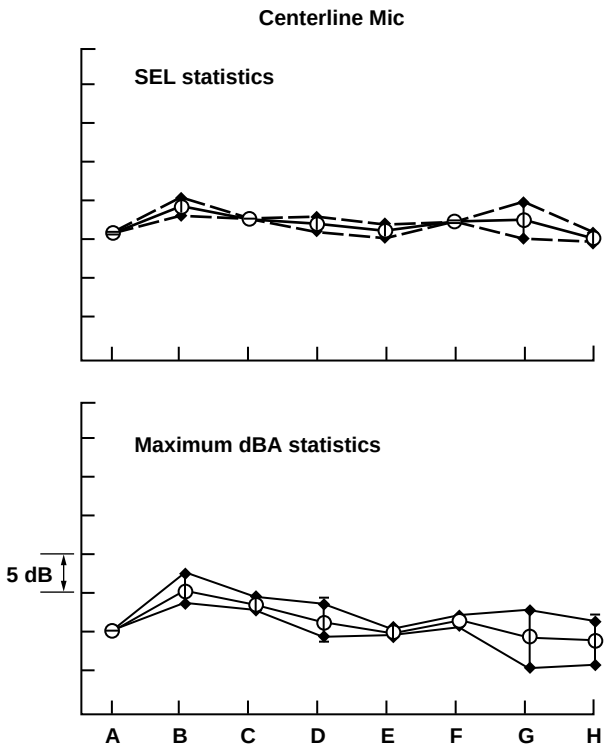


*Figure 22. SEL dB and dBAmax statistics for all the groups tested at the centerline mic #2. (Note: The baselines and the scales are the same.) Open circles are for the mean, horizontal bars for the standard deviation, and diamonds for the range.*

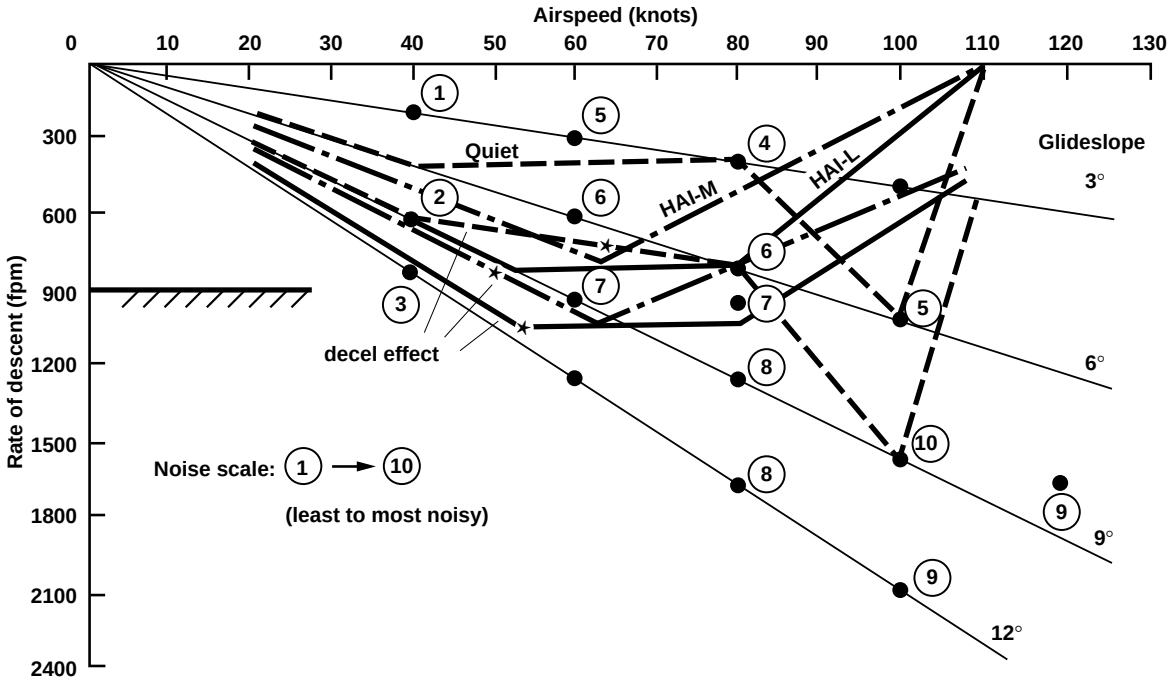


*Figure 23. Tested noise-abatement flight profiles shown in the plane of airspeed vs. rate of descent, with and without considerations of deceleration effect.*

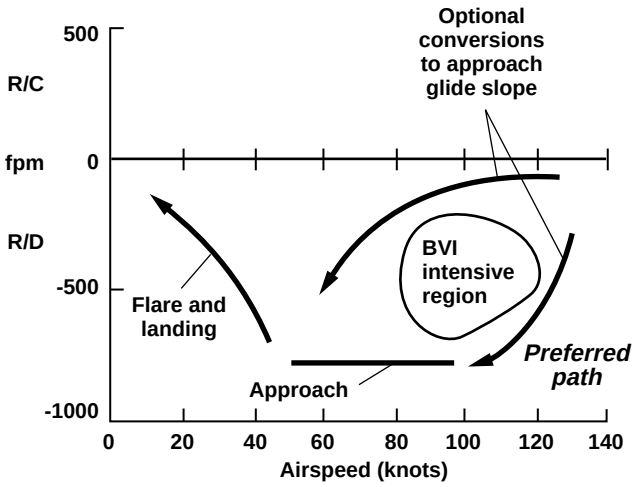


*Figure 24. Preferred flightpath to avoid BVI intensive region.*

# REPORT DOCUMENTATION PAGE

*Form Approved*
*OMB No. 0704-0188*



| 1. AGENCY USE ONLY *(Leave blank)* | 2. REPORT DATE | 3. REPORT TYPE AND DATES COVERED |
|---|---|---|
| | September 1995 | Technical Memorandum |

**4. TITLE AND SUBTITLE**

Acoustic Flight Tests of Rotorcraft Noise-Abatement Approaches Using Local Differential GPS Guidance

**5. FUNDING NUMBERS**

505-59-36

**6. AUTHOR(S)**

Robert T. N. Chen, William S. Hindson, and Arnold W. Mueller*

**7. PERFORMING ORGANIZATION NAME(S) AND ADDRESS(ES)**

Ames Research Center
Moffett Field, CA 94035-1000

**8. PERFORMING ORGANIZATION REPORT NUMBER**

A-950102

**9. SPONSORING/MONITORING AGENCY NAME(S) AND ADDRESS(ES)**

National Aeronautics and Space Administration
Washington, DC 20546-0001

**10. SPONSORING/MONITORING AGENCY REPORT NUMBER**

NASA TM-110370

**11. SUPPLEMENTARY NOTES**

Point of Contact: Robert T. N. Chen, Ames Research Center, MS 211-2, Moffett Field, CA 94035-1000; (415) 604-5008
*Langley Research Center, Hampton, Virginia.

**12a. DISTRIBUTION/AVAILABILITY STATEMENT**

Unclassified-Unlimited
Subject Category – 05

Available from the NASA Center for AeroSpace Information,
800 Elkridge Landing Road, Linthicum Heights, MD 21090; (301) 621-0390

**12b. DISTRIBUTION CODE**

**13. ABSTRACT *(Maximum 200 words)***

This paper presents the test design, instrumentation set-up, data acquisition, and the results of an acoustic flight experiment to study how noise due to blade-vortex interaction (BVI) may be alleviated. The flight experiment was conducted using the NASA/Army Rotorcraft Aircrew Systems Concepts Airborne Laboratory (RASCAL) research helicopter. A Local Differential Global Positioning System (LDGPS) was used for precision navigation and cockpit display guidance. A laser-based rotor state measurement system on board the aircraft was used to measure the main rotor tip-path-plane angle-of-attack. Tests were performed at Crows Landing Airfield in northern California with an array of microphones similar to that used in the standard ICAO/FAA noise certification test. The methodology used in the design of a RASCAL-specific, multi-segment, decelerating approach profile for BVI noise abatement is described, and the flight data pertaining to the flight technical errors and the acoustic data for assessing the noise reduction effectiveness are reported.

| 14. SUBJECT TERMS | 15. NUMBER OF PAGES |
|---|---|
| Acoustics, Noise abatement approaches, Differential GPS | 38 |
| | 16. PRICE CODE: A03 |

| 17. SECURITY CLASSIFICATION OF REPORT | 18. SECURITY CLASSIFICATION OF THIS PAGE | 19. SECURITY CLASSIFICATION OF ABSTRACT | 20. LIMITATION OF ABSTRACT |
|---|---|---|---|
| Unclassified | Unclassified | | |